Sox17 controls emergence and remodeling of Nestin-expressing coronary vessels

Sara González-Hernández, PhD[1,#], Manuel J. Gómez, PhD[1,2], Fátima Sánchez-Cabo, PhD[1,2], Simón Méndez-Ferrer, PhD[3], Pura Muñoz-Cánoves, PhD[1,4] and Joan Isern, PhD[1,4*]

[1]Centro Nacional de Investigaciones Cardiovasculares (CNIC). Madrid, Spain; [2]Bioinformatics Unit, CNIC, Madrid, Spain; [3]WT-MRC Cambridge Stem Cell Institute and NHS-Blood and Transplant, Cambridge, UK; [4]Cell Biology Group, Department of Experimental and Health Sciences, Pompeu Fabra University (UPF), Barcelona, Spain

[#] Current address: Laboratory of Stem Cell and Neuro-Vascular Biology, National Heart, Lung, and Blood Institute, National Institutes of Health, Bethesda, MD, USA.

Running title: Sox17 in developmental coronary arteriogenesis

Subject terms:
Developmental Biology
Vascular Biology
Coronary Circulation
Genetically Altered and Transgenic Models
Gene Expression and Regulation

Address correspondence to:

Dr. Joan Isern
Vascular Pathophysiology Area
Centro Nacional de Investigaciones Cardiovasculares Carlos III (CNIC)
Melchor Fernandez Almagro 3,
28029 Madrid, Spain.
Jisern@cnic.es

ABSTRACT

Rationale: The molecular mechanisms underlying the formation of coronary arteries during development and during cardiac neovascularization after injury are poorly understood. However, a detailed description of the relevant signaling pathways and functional transcription factors regulating these processes is still incomplete.

Objective: The goal of this study is to identify novel cardiac transcriptional mechanisms of coronary angiogenesis and vessel remodeling by defining the molecular signatures of coronary vascular endothelial cells (EC) during these complex processes.

Methods and Results: We demonstrate that *Nes-gfp* and *Nes-CreER^{T2}* transgenic mouse lines are novel tools for studying the emergence of coronary endothelium and targeting sprouting coronary vessels (but not ventricular endocardium) during development. Furthermore, we identify *Sox17* as a critical transcription factor upregulated during the sprouting and remodeling of coronary vessels, visualized by a specific neural enhancer from the *Nestin* gene that is strongly induced in developing arterioles. Functionally, genetic inducible endothelial deletion of *Sox17* causes deficient cardiac remodeling of coronary vessels, resulting in improper coronary artery formation.

Conclusions: We demonstrated that Sox17 transcription factor regulates the transcriptional activation of *Nestin*'s enhancer in developing coronary vessels while its genetic deletion leads to inadequate coronary artery formation. These findings identify Sox17 as a critical regulator for the remodeling of coronary vessels in the developing heart.

Keywords:
Coronary vascular development; nestin neural enhancer; transcriptional regulation; Sox17; arteriovenous (AV) specification.

Nonstandard Abbreviations and Acronyms:

CoronEC	Coronary Endothelial Cells
EMSA	Electrophoretic Mobility Shift Assay
MCEC	Mouse Cardiac Endothelial Cells
RaOp	Ragged Opossum
TF	Transcription factor

INTRODUCTION

The muscular walls of the adult heart contain a deep network of microvascular endothelium, organized through higher-order vessels into the main coronary arteries (CA) and veins (CV). This highly branched system is assembled during development from a relatively simple vascular plexus, which extends by sprouting angiogenesis from multiple sources and penetrates the ventricular myocardium[1,2]. Upon connecting with the aortic lumen, the primitive plexus already in place is further reorganized due to increasing shear stress forces, provided by the nascent intracoronary flow[3], ultimately maturing in the hierarchical definitive arteriovenous coronary vasculature. Understanding the essential molecular signals regulating the patterning, assembly, and remodeling of coronary vessels is of great interest given the high incidence of cardiovascular disease and congenital coronary anomalies[4]. Moreover, genetic programs activated during neovascularization or in response to pathological ischemia often recapitulate morphogenetic programs from healthy development; thus, identifying the critical molecular regulatory factors at the molecular level in coronary development might pave the ground to design novel strategies to improve revascularization and intrinsic cardiac repair.

Functional analysis of genomic regulatory regions has proven to be a potent tool to identify the cell's underlying transcriptional activating machinery, as enhancers often integrate multiple upstream signals to regulate gene expression in a cell type-specific manner. In this work, we have taken advantage of *Nestin's* neural enhancer-driven transgenic mouse lines as novel tools for studying transcription factors (TFs) upregulated during sprouting and remodeling of coronary vessels.

The intermediate filament *Nestin* was originally identified as an abundant protein in rat neuroepithelial progenitors[5], although its tissue expression domains are highly dynamic and not entirely restricted to the neurogenic lineages[6]. Although the endogenous expression of a gene is determined by the combined activity of multiple enhancers proximal or even far away from its locus, each enhancer might reveal or act as a proxy of the discrete transcriptional pathway that ultimately activates it. Several independent regulatory elements have been identified in the *Nestin* (*Nes*) locus[7], with the best characterized being a strong transcriptional neural enhancer located in the second intron of the rat gene[8]. This intronic enhancer, in conjunction with 5,8-kb of the proximal promoter region, was initially used to generate a *Nestin*-GFP (*Nes-gfp* onwards) transgenic mouse line driving the expression of a fluorescent green protein (GFP) reporter, aimed to reproduce its particular pattern of expression in the brain[9]. Intriguingly, vascular ECs in some instances (like abnormal vasculature from glioma tumors) have also been reported to express *Nestin*, suggesting a related local signaling in the vessel environment able to activate the enhancer. Indeed, the *Nes-gfp* allele has been used to effectively visualize tumor angiogenesis in xenogeneic models[10]. Given the organ-specific characteristics of vascular beds, it is unclear whether this enhancer would also be induced in the heart vasculature or during coronary formation. In bone marrow, a combination of surface markers with GFP reporters of different brightness has been used to prospectively separate arterial ECs[11] .

In the heart, some markers and transgenic mouse strains based on them have been previously applied to study the coronary endothelial and endocardial lineages, such as *Apelin-nLacZ*, *Aplnr-CreER, Fabp4-Cre*, or *Nfatc1-Cre*, *Npr3-CreER* respectively. Characterizing additional fluorescent reporter transgenic alleles that may label coronary angiogenesis would improve imaging and would allow examination of unfixed cells. Here we have leveraged the activation of *Nestin*'s neural enhancer specifically in vascular ECs of the murine embryonic heart to study coronary formation at unprecedented resolution. By combining *Nes-gfp* reporter and *Nes-CreER^{T2}* driver (both randomly integrated transgenic alleles) with other markers, we have been able to separate and profile molecularly the distinct cardiac EC subtypes, including endocardial, prospective arterial and venous endothelial cells. We identified *Sox17*, a member of the SoxF subgroup of the SOX (SRY related-HMG box) family of transcriptional regulators, to be highly enriched in *Nestin*-labelled ECs. Coronary EC-specific inactivation of *Sox17* in the embryonic heart leads to defective coronary vascularization and a lack of CA formation, reinforcing its critical role only for the proper arterial remodeling of the coronary vasculature.

METHODS

Detailed methods are available in the **Online Data Supplement** section.

Data availability.

The data that support the findings of this study are available from the corresponding author upon reasonable request. Please see the **Major Resources Table** in the Supplemental Materials for a complete list of the Research materials.
All sequencing datasets in this article are deposited in the International Public Repository, Gene Expression Omnibus (GEO) database, under accession code GSE147128.

RESULTS

The Tg(Nes-gfp) allele robustly labels the emerging coronary vascular plexus and the arteriogenic remodeling zones

Previous studies in bone marrow using the transgenic *Nes-gfp* mice have revealed a dual *Cxcl12*-expressing population, that comprises both GFP+ vascular endothelial and vessel-associated GFP+ stromal cells[12, 13]. Given the important role of the *Cxcl12* signaling axis in coronary development and injury-induced arteriogenesis[3, 14], we speculated that this same GFP reporter would be transiently activated in nascent coronary endothelial cells (coronEC) during cardiac development, reminiscent of a shared regulation or conserved functions. Because the expression pattern of the *Nes-gfp* allele at those stages (and specifically within the vascular compartment) has not been carefully inspected, we focused our attention on studying the endothelial lineage. We observed that the *Nes-gfp* reporter efficiently labeleld developing coronEC in embryonic hearts (**Figure 1**). Indeed, we confirmed that the sprouting GFP+ cells were of *bona fide* endothelial nature by: 1) their overlap with *Tie2*-lineage-traced cells (which was genetically marked with tomato reporter and the pan-endothelial *Tie2-cre* driver, which also labels the inner trabeculated endocardium (**Figure 1A**); and 2) by co-expression in the nucleus of the endothelial-specific Erg marker (**Online figure IA**). We could directly observe endogenous GFP signal from fresh and fixed intact hearts, which when combined with whole-tissue clearing (using CUBIC method with confocal microscopy, **Online figure IB**), allowed us to reconstruct the early primitive vessel arrangement during the E12.5-P1 developmental window at unprecedented volumetric resolution (**Figure 1B** and **1C**). We acquired z-stacks composed of multiple consecutive single optical slices (up to ~500-□m thick), reaching the internal cardiac chambers with a high level of detail and preserving the vascular structure (**Online figure IC**). The coronary arteriogenic remodeling zones, throughout the left anterior ventricle, could be easily appreciated (**Figure 1B**, arrowheads). At later stages, the maturing CAs were brightly delineated by GFP+ expression, including neonatal *Nes-gfp* hearts (white asterisks). Deeply remodeling regions coalescing into arterioles from the posterior side, were also visible (**Figure 1C**, open arrowheads). Considering that *Nes-gfp* allowed visualizing cardiac vasculature with high resolution and especially big arteries during embryonic and neonatal stages, we crossed *Nes-gfp* mice with the mice *null* for the *Cxcl12* allele. Indeed, compound transgenic *Nes-gfp; Cxcl12*^{KO} hearts at E17.5 showed (without the need of further stainings) a persistent unremodeled coronary plexus and the complete absence of the left CA (**Online figure ID**), as has it been previously reported[3, 15]. Thus, this allele can be useful to directly reveal the normal pattern and, specifically, abnormalities in fetal coronary plexus formation and subsequent remodeling and maturation of CAs.

Focusing on the early sprouting phase at E12.5-13.25 (**Figure 1A-1D**), we could observe fine angiogenic processes of dorsal coronECs invading the myocardial wall proximal to the sinus venosus (SV) region and extending towards the intraventricular septum (IVS) (arrowheads, boxed regions). We observed that the *Nes-gfp* allele was activated in ventral coronECs (sprouting laterally towards the surface of the primitive left ventricle), within the anterior ventricular groove (VG) region (**Figure 1B** and 1D, arrowheads), which have been suggested to originate from endocardial progenitors[16, 17]. Therefore, with the detailed analysis of hearts from *Nes-gfp* Tg mice, we confirmed that most of the primitive endothelial sprouts have the promoter/neural enhancer that controls the GFP reporter expression activated in coronary vessels during the angiogenic phase, regardless of the different origins of the primitive plexus.

We then asked whether we could track the deeper ventricular coronary vessels during the remodeling phases. As reported[1, 18], we observed that GFP+ coronECs expand quickly subepicardially, covering the dorsal surface of the heart and penetrating the myocardial wall, and the septum (**Figure 1C** and **1E**). The reporter expression remained absent in the ventricular endocardium at the analyzed stages (**Online figure IA** and **IE**). Interestingly, the vessels sprouting towards, and within, the intramyocardium upregulate the GFP signal (**Figure 1E**, boxed area, arrowheads). At late embryonic stages (E16.5), the venous subepicardial plexus (**Online Figure IE**, arrowheads) showed downregulated GFP expression, while the endocardium in the trabeculae was still negative (**Online figure IE**, orange asterisks).

Taken together, these data suggest that signals activating the *Nes* promoter/neural enhancer are present in all sprouting ECs, regardless of the origin (SV or ventricular endocardium). At

midgestation, because of the dynamic relative expression levels driven by the activity of the neural enhancer in coronECs, subepicardial vessels progressively downregulate GFP expression whereas the reporter is highly maintained in intramyocardial plexus and subsequent remodeled CAs.

Discrimination of coronary from endocardial endothelium in developing hearts based on endomucin and Nes-gfp

Considering that the *Nes-gfp* allele specifically labeled coronECs and was barely expressed by endocardial cells from the ventricular chambers (which otherwise express high levels of endomucin (**Online figure IIA-IIC**), we aimed to separate both endothelial subsets from the same hearts. We enzymatically-dissociated cardiac cells from dissected *Nes-gfp*+ ventricles. After excluding debris/non-viable cells and red blood/hematopoietic cells (by DAPI/CD45/Ter119 expression), we FACS-isolated viable CD31+ ECs, separating them based on endomucin (Emcn) surface levels and endogenous GFP fluorescence (**Figure 2A**). Analysis by qRT-PCR of these isolated sub-populations confirmed the high purity of each subset, given the reciprocal enrichment in mRNA expression of the coronary EC-specific markers *Apelin* (*Apln*) and *Fabp4* in the Emcn(low)/*Nes*-GFP(+) vessels, and the endocardial EC markers *Npr3* and *Emcn*, respectively (**Figure 2B**). Thus, the combination of GFP reporter with Emcn staining shows mutually exclusive expression pattern of these EC subpopulations (**Figure 2D** and **Online figure IIC**). This strategy allowed us to quantify at the cellular level the dynamic expansion of the ventricular coronary vascular compartment by FACS (**Figure 2C**). During the E13-5-17.5 window, ECs of the primitive coronary plexus increased more than 3-fold. Conversely, the endocardial compartment is dominant at E13.5 (coinciding with the big and intricate surface of the trabeculae) and is progressively reduced, consistent with compaction and thickening of the vascularized ventricular myocardial walls.

Considering that the most superficial coronary plexus downregulated the GFP expression from E13.5 onwards (**Online figure IIC** and **IE**), we expected that, after remodeling, the reporter should be maintained in intramural capillaries and CAs, but not in the subepicardial prospective CVs. Whole-mount and tissue section immunostainings of *Nes-gfp*+ hearts at 17.5-18.5 revealed that the microvasculature and arterial ECs maintained high levels of GFP reporter whereas CVs (Emcn+) showed decreased levels of GFP (**Figure 2E** and **2F**).

Collectively, the combination of *Nes-gfp* reporter with CD31 and Emcn markers, which display non-overlapping expression patterns, allow us to discriminate between ventricular endocardium (CD31+Emcn+GFP-) from coronary vessels (CD31+Emcn$_{low}$GFP+) with high reliability from the same pool of hearts during development.

Lineage tracing with Tg(Nes-CreER^{T2}) labels coronary vessels but not endocardial cells in developing ventricles

Based on our observation of the *Nes-gfp* allele cardiac expression pattern, we next investigated whether the tamoxifen-inducible *Nes-CreER^{T2}* transgenic line (*Nes-CreER* onwards), developed initially to follow postnatal neurogenesis[19], could target embryonic coronary endothelium. Both *nes*-based transgenic lines have in common the presence of the same regulatory neural-specific enhancer element from *Nestin's* second intron[20]; however, the *Nes* promoter region is only present in *Nes-gfp* allele and not in *Nes-CreER* driver (**Online figure IID**). To genetically label cells expressing *Nes-CreER* and their descendants, we crossed it with the *R26-tomato* reporter line, which expresses the fluorescent tdTomato (tom) reporter upon Cre-mediated recombination.

To determine if we could label the earliest superficial vessels arising in the dorsal ventricular wall around E11.5[1], we used tamoxifen (TMX) to induce expression of *Nes-CreER* at E10.5 and analyzed the labeled cells 48h later. As hypothesized, we efficiently labeled the primitive coronary plexus, being able to visualize tom+ primitive endothelial tubes in whole-tissue clarified hearts, extending throughout the dorsal ventricular region (**Figure 3A** and **3B**). Furthermore, induction of labeling during the E10.5-E12.5 window allowed tracing most coronECs (including intramyocardial capillaries/arteries and subepicardial veins) but not the ventricular endocardium. Thus, whole-mount confocal imaging of cleared hearts at E15.5 showed the same pattern of tom+ coronary vessels upon induction at both stages (**Online figure IIIA** and **IIIB**). In sections, the main difference found when inducing at E10.5 or E12.5 was the number of traced ECs in the IVS (**Online figure IIIC** and **IIID**).

We further crossed *Nes-CreER* with the *Nes-gfp* line to concurrently visualize *Nes*-GFP+ cells and the (tom+) *Nes*-lineage. In **Online figure IIIE-IIIG**, we showed a whole-mount triple transgenic E18.5 heart, TMX-induced at E10.5, where remodeled coronary vessels and capillaries were traced by tomato expression. Vascular smooth muscle cells surrounding the CA and many pericytes also expressed the *Nes-gfp* reporter (quantified by FACS at E17.5, **Online figure IIIH**). Taking together, these date demonstrate that *Nes-CreER* line is more restricted in marking coronECs at the stages examined.

Considering the dynamism of *Nes-gfp* expression and its downregulation in subepicardial ECs during the remodeling phase (**Online figure IE** and **Figure 2E**), we predicted that the *Nes-CreER* driver could be used to selectively mark intramyocardial vessels, including capillaries and prospective arteries, and excluding subepicardial veins and ventricular endocardium. Immunostaining with estrogen receptor (ESR) antibody as a surrogate of *Nes-CreER* expression showed that the *NesCreER*-expressing cells were confined to the intramyocardial wall and not to the subepicardial layer nor the endocardium, in E15.5 embryonic heart sections (**Online figure IVA**). Subsequently, we quantified the traced cells from E17.5 hearts by flow cytometry after TMX induction at E12.5 or E15.5 (**Figure 3C**). TMX-induced hearts at E12.5 showed that 72% of the tom+ population had endothelial lineage identity (CD31+), including prospective arteries and veins, based on Emcn expression levels (**Figure 3D**). In contrast, fate-mapping inducing with a lower dose of tamoxifen at E15.5 showed that more than 90% tom+ cells were intramyocardial ECs, with much lower coverage (from 30% to 7% of recombined cells) of the venous subpopulation (CD31+ tom+ Emcn+) (**Figure 3E**).

To further investigate these two tracing conditions, we performed confocal microscopy of longitudinal cardiac sections (**Figure 3F** and **3G**). We found that the *Nes-CreER* allele could mark all coronECs (both subepi- and intramyocardial layers, black and green bars, respectively) when induced at E12.5 (**Figure 3F**). We also measured in sections the colocalization between tom+ cells and Isolectin B4 marker in the ventricular walls (**Online figure IVB-IVC**). Conversely, when inducing with the lower TMX dose at E15.5, only capillaries and arteries from the deeper ventricular wall became labeled, with most of the subepicardial vessels escaping recombination and remaining tom-negative (**Figure 3G**). Moreover, during the E10.5-E15.5 induction windows, we could not detect endocardial cells labeled in the ventricles, confirming its coronary vessel specificity. We also reported in **Online figure IVD** the maximal projection of whole-mount E17.5 heart showing at high resolution tom+ CAs and capillaries (ventral side), whereas CVs (identified with Emcn in the dorsal side) escaped recombination.

Overall, these data strongly suggest that *Nes-CreER* driver is a useful tool for specific lineage tracing of embryonic coronECs, and primarily to drive coronary-restricted excision of conditional floxed alleles to carry out functional genetic studies.

Developmental profiling of endocardial and coronary endothelial cells

Taking advantage of the novel genetic tools that we have characterized to label specific subsets of cardiac endothelium, we aimed to reveal the dynamic transcriptional changes occurring in coronECs during plexus emergence and maturation. We determined the global transcriptomic profiles between highly purified embryonic endocardium and coronary endothelium by using the cell sorting strategy. Primary cardiac ECs were isolated by FACS from developing hearts based on their distinctive phenotypes at two selected stages: during active sprouting (E13.5), and when immature plexus is undergoing extensive remodeling (E17.5). Starting from dissociated *Nes-gfp* fetal hearts, by using the pan-endothelial marker CD31, endomucin (Emcn), and GFP levels, we separated bona fide coronECs (marked by GFP expression), from ventricular endocardium (which was GFP-negative and presented higher Emcn surface staining, **Online figure VA**).

Four biological replicates were used for E13.5 stage and two replicates for E17.5 (**Figure 4D**). Expression of coronary plexus-enriched versus endocardial-enriched genes were represented in FPKM in **Online figure VB**. Moreover, the expression levels of a selection of marker genes confirmed that transcriptomic profiles were specific of vascular endothelium and that contamination from other population, such as hematopoietic cells, cardiac fibroblast or cardiomyocytes, has been avoided (**Online figure VC**). We identified 7,519 and 8,925 genes differentially expressed (p_{adj}<0,05) between endocardium and coronECs, and also between sprouting (E13.5) and remodeling phase

(E17.5), respectively (**Online figure VD**). These genes were clustered into 5 groups based on their expression pattern (**Figures 4A** and **4B**). Clusters I and V corresponded with genes exclusively expressed in coronECs or endocardium, respectively, indicating specificity for each endothelial subset independently of the developmental stage. Conversely, clusters III and IV contained genes overexpressed from sprouting to remodeling phase regardless of the endothelial subtype. Finally, we focused our attention, however, on genes differentially expressed between coronary plexus and endocardium whose expression increased from the angiogenic to the remodeling phase (cluster II), as this implied that these genes could be necessary not only for the development of the primitive plexus, but specially for the posterior remodeling and maturation. Pathway analyses of the DEG are depicted in a circular GOplot showing some functions associated with them (**Figure 4C**).

Among all candidates found in Cluster II, we focused on genes sharing the same expression profile than GFP reporter, with particular interest on TFs that could be simultaneously regulating the reporter activation in these cells and having a relevant role in arterial specification and remodeling (**Figure 4E**).

Gene expression profiling of coronary arterial- vs venous-enriched ECs

Next, based on our genetic ability to selectively label intramyocardial vessels (**Figure 3G**), we combined this specific tracing with the *Nes-gfp* /emcn strategy in order to isolate from the same hearts the three subsets of ECs: endocardium, intramyocardial arteries/capillaries and subepicardial veins. We dissociated pools of ventricles from E17.5 *Nes-gfp; Nes-CreER; R26-tom* hearts (TMX-induced at E15.5), and based on Emcn and GFP levels, we segregated by FACS: 1) endocardial ECs ($CD31^{+}Emcn^{high}GFP^{low}$) from the rest of coronECs ($CD31^{+}Emcn^{low}GFP^{+}$). Then, the coronary vessels were further split in: 2) tom+ cells (fate-mapped arterial and capillaries-enriched subset), and 3) the remaining more heterogeneous tom^{-} GFP^{low} fraction (enriched in prospective subepicardial venous ECs) (**Online figure VE** and **VF**). Finally, we performed bulk RNAseq from the three isolated cardiac endothelial subtypes.

Principal component analysis (PCA) showed that we succeeded in sampling the 3 main EC populations, which occupied separated coordinates in the bidimensional plot (**Figure 5A**). Because we had previously demonstrated the high efficiency separating endocardium versus coronECs, we also represented in **Online Figure VG** and **VH** the expression of selected arterial-specific (*Cxcr4, Dll4, Gja5*) and venous-enriched genes (*Aplnr, Edn1, Nr2f2*) between arterial- and venous-enriched subpopulations. When compared together, the arterial- and venous-enriched subsets were transcriptionally distinct. Circular GOplot in **Figure 5B** showed differentially expressed genes between both populations. **Figure 5C** presented previously unreported arterial-enriched genes compared with subepicardial veins and ventricular endocardium, including *Stmn2, Rgs5, Art3, St8sia6,* and *Alox1*2. Interestingly, although the expression pattern in veins were slightly closer to the endocardium, we could identify not only differentially expressed genes compared with arteries (*Rcn3, Cpe, Dlk1, Dcn, Pos*t) but also genes that were exclusively expressed in the venous population, including *Ogn, Dpt, Col1a1* (**Figure 5D**). Finally, we also compared in volcano plots differentially expressed genes between arterial coronECs and endocardial ECs (**Figure 5E**), i.e., Vwf*, Nrg1 and Cldn11* in the endocardial side and *Kitl, Nes, Prdm1 and Sox17* as arterial-specific.

Thus, we have established a novel method to separate different subsets of cardiac ECs from the same hearts based on *Nestin*-related transgenic lines. Bulk RNAseq at different stages allowed us to analyze differential expression patterns not only between subpopulations, but also to track the maturational trajectories for each endothelial subtype. Ultimately, this strategy allowed us to identify novel potential factors involved in sprouting and/or subsequent remodeling process and arterio-venous specification.

Sox17 is upregulated in prospective coronary arteriolar endothelium

From both RNAseq profiling results, we focused our attention on discovering potential TFs that could mediate the activation of the *Nes-gfp* enhancer in developing coronary vessels, but not in the ventricular endocardium, where expression of this reporter is very low. The SoxF subgroup of TFs have been previously implicated in vascular development and lymphangiogenesis, as well as arterial specification identity[21, 22]. We found that all 3 SoxF members (*Sox7,17,18*) were expressed at diverse

levels in coronECs, but only *Sox17* had an expression pattern and kinetics similar to the *Egfp* mRNA, as proxy of activation of the *Nes-gfp* allele (**Figure 6A**). Moreover, at E17.5, Sox17 expression, like that of *Nes-gfp*, was significantly higher in the sorted arterial population, compared to venous and endocardial cells (**Figure 6B**). We validated by immunostaining the coexpression of Sox17 protein in GFP+ vessels and confirmed strong nuclear reactivity that correlated with increasing GFP levels. Remarkably, in E11.5 cardiac sagittal sections, the first immature coronary sprouts in the anterior side of the ventricular wall, and extending dorsoventrally behind the epicardial layer, already displayed nuclear Sox17+ expression, which correlated with the onset of the *Nes-gfp* activation in the invading ventricular wall vascular plexus (**Figure 6C**). Later on, coinciding with the downregulation of the GFP reporter in prospective veins, we quantified Sox17 expression by immunofluorescence in sections and confirmed a robust upregulation at E13.5, concomitant with a progressive GFP expression increase, in the intramyocardial plexus (**Figure 6D** and **6E**). It has been reported that some endocardial cells activate Sox17 in the anterior left ventricle, close to the interventricular septum[16]. We confirmed this in E13.5 whole-tissue hearts and found co-expression of Sox17 and GFP reporter in anterior ventricular groove blood island-like structures. We also detected sparse cells in the Emcn+ endocardial layer with nuclear Sox17 staining in both ventricles. Intriguingly, most of the Emcn+ Sox17+ endocardial cells were located at the base of the trabeculae (**Online Figure VIA-VIC),** apparently sprouting from the lumen of the ventricle into the intramyocardial wall, giving rise to structures resembling the described endocardial flowers[23]. We suggest that these endocardial cells that invade the myocardium and contribute to the coronary vessels should activate Sox17 for this transition. Interestingly, the endocardial-derived cells that upregulate Sox17 in the base of the trabecule also activate *Nes-gfp* reporter, showed in sections in E16.5 hearts (**Online figure VID**).

Finally, in more advanced stage hearts, at the end of the remodeling phase, whole-mount staining showed the maintenance of Sox17 expression in bright GFP+ arterioles (**Figure 6F**). Because of the tight colocalization observed between *Sox17* and GFP-expressing cells, we propose that this TF may directly regulate *Nestin* neural enhancer in coronECs during sprouting phase and be therefore involved in the remodeling of intramyocardial vessels.

Identification of an intronic Nes transcriptional enhancer with Sox17-dependent activity in coronary endothelium

To determine if our candidate *Sox17* could be responsible for the cardiac endothelial induction of the *Nes-gfp* and *Nes-CreER alleles*, we searched for genomic evolutionary conserved regions (ECR) at *Nestin*'s locus. The second intron is the common element present in both transgenic constructs and could be responsible for the extraneural enhancer activity in coronECs. We found a 1,44kb region located at the 3' end of the intron which contains two well-conserved sequence stretches (CR1 and CR2) with predicted SOX binding motifs (**Figure 7A**). The SOX family of TFs share similar DNA binding domains, so distinct members can potentially recognize the same canonical sites. Using a more restrictive matrix, the predicted SOX sites identified in both CR regions displayed also a high score in jaspar for Sox17 binding, with absolute nucleotide conservation across species in the critical positions of the motif. Multiple ETS sites with conserved sequences where also identified nearby.

To validate whether the predicted SOX motifs in CR1/2 could represent a *bona fide* binding sites for Sox17, we performed electrophoretic mobility shift assays (EMSA) with nuclear extracts from a Sox17-overexpressing cardiac endothelial MCEC line (**Online figure VIIA**). Analysis by qPCR of different genes showed that MCEC expressed a mix of markers for the different ECs subpopulations (*FoxC1, Cdh11*, *Nr2f2, Cxcl12, Nes, Unc5b,* among others) but they did not express any of the SoxF TFs that are present in the developing coronary vasculature *in vivo* **(Online figure VIIB)**. Both CR1 and CR2 labeled oligos (red and green, respectively) were bound by the extract, but the CR1 element showed stronger specific binding, which could in turn be displaced by excess of unlabeled probe. In contrast, excess of the same probe with mutated nucleotides in the binding motif did not compete as efficiently (**Figure 7B**).

To explore whether this enhancer could be functional in cardiac ECs and transactivate a heterologous reporter, we performed transient luciferase reporter assays with the full-length intact second intron (i2_full) or with deleted fragments (ΔCR1, ΔCR2) of the intron in MCEC overexpressing Sox17 protein **(Figure 7C** and **Online Figure VIIC).** Deletion of both CR in the *Nes*

neural enhancer reduced the luciferase activity by 5-fold, although residual reporter activity remained, similar to controls not overexpressing Sox17. Because *Sox18* was also differentially expressed between *Nes*-GFP+ coronECs and GFP- endocardium (**Figure 6A**), we also tested if this TF could be able to activate the enhancer. We showed that there were no differences in the reporter activity with or without overexpressing *Sox18* (**Figure 7C**). Co-expression of both Sox17 and Sox18 did not have an additive effect, but rather reduced the luciferase reporter induction (**Online figure VIID**). In addition, we generated a double transgenic doxycycline-inducible *Sox17* MCEC clone containing *Nestin*'s second intron fused to tomato reporter construct. By increasing doxycycline concentration, we could see the progressive induction of tomato reporter expression (**Online figure VIIE-VIIG**).

Collectively, these results demonstrate that in coronECs, Sox17 interacts with the SOX motif present in the CR1 and CR2 of the *Nestin* promoter, showing specificity for the CR1. This interaction is sufficient for activation of the *Nestin* neural enhancer *in vitro*. Altogether, Sox17 TF is directly regulating *Nestin* neural enhancer in coronECs but not in the ventricular endocardium, suggesting a potential role in sprouting immature plexus prior to arterial specification.

Sox17 mediates the correct formation and subsequent remodeling of the coronary vasculature

We further performed HUVECs tube formation assay to determine whether the absence of SoxF TFs could affect the angiogenic capacity of ECs. HUVECs were co-transfected with a plasmid-expressing the Sox18 *Ragged opossum* variant, which acts in a dominant-negative for all SoxF family members[24]. We concluded that transfection of HUVECs with $Sox18^{RaOp}$ resulted in a significant decrease in the number of loops and branching points in the tube formation, compared with control situation (**Figure 7D** and **7E**).

After demonstrating that *Sox17* regulated *Nestin* enhancer in ECs *in vitro*, we next decided to deleted *Sox17 in vivo* specifically in coronary vessels at the time they start to develop. To overcome the lethality of global *Sox17* null embryos, we conditionally deleted *Sox17* within the endothelial lineage, taking advantage of the *Nes-CreER* driver to precisely test *Sox17* function in Nes+ cells, and to restrict excision primarily to coronary vessels, thus avoiding indirect effects from the endocardium. We generated *Sox17* conditional mutant embryos ($Sox17^{cKO}$) carrying the Rosa26-*tomato* reporter allele to follow recombined cells, and also carrying the *Nes-gfp* reporter allele to directly inspect any coronary network misspatterning. Tamoxifen-induced deletion of the $Sox17^{floxed}$ was performed at E10.5 and E12.5 (**Figure 8A**) to target the earliest coronary sprouting cells from the SV at E11.5 and analyzed the vascular phenotype in the coronary network. E16.5 *Nes-CreER;*$Sox17^{floxed}$ embryos only had a few remaining ventricular Sox17+ cells compared with WT embryos (not shown), confirming the effective deletion within the E10-E12.5 window. **Figure 8** and **Online figure VIII** show that $Sox17^{cKO}$ hearts had severe coronary remodeling defects, with abnormal CA formation and retarded unremodeled coronary plexus, compared to stage-matched control WT littermates. The penetrance of the phenotype was variable, but most of the mutant embryos presented coronary defects, with the most affected ones showing overt lack of the main anterior left coronary artery (**Figure 8B-C** and **Online figure VIIIA**) and in fewer cases, also complete absence of the posterior right artery (Figure 8D). By contrast, CVs remain unaffected (**Online Figure VIIIB**). The connections of both left and right coronary arteries appared to form normally in most of the $Sox17^{cKO}$ hearts, as assessed by deep confocal optical reconstruction of the proximal aortic region (**Online Figure VIIIC**). In the mutants, we further observed an expansion of Sox17+ tom- cells, possibly derived from activated, non-recombined endocardium that had incorporated into the plexus to compensate for the vascular defects (**Figure 8D** and **Online figure VIIID**, boxed area), indicating that Sox17 was necessary for the arteriogenic maturation of the primitive plexus. However, even with such ectopic overexpression of Sox17 in ventricular endocardium, mutant hearts fail in the correct remodeling to give rise to proper CAs.

Collectively, we propose that contrary to what had been described in other tissues[24], expression of the other SoxF factors (*Sox7* and *Sox18*) in coronECs is not sufficient to compensate for the lack of *Sox17* in this developing plexus. More importantly, our data reveal that Sox17 has a crucial role in initial steps of coronary plexus development and not only in the subsequent remodeling of CAs.

DISCUSSION

In the present study we exploited a novel set of cardiac genetic tools, including both the *Nestin*'s neural enhancer-driven *Nes-gfp* and *Nes-CreER^{T2}* Tg mouse lines, to explore the signals controlling the formation and maturation of the coronary endothelium. We identified the TF Sox17 as a critical regulator for the remodeling of coronary vessels. In fact, its genetic deletion led to inadequate coronary artery formation.

The same intronic enhancer -shared by both lines used here- has been the critical element (in conjunction with variable regions of *Nestin's* proximal promoter region) to generate a number of *Nestin*-based Tg reporter lines lines, mostly for neurogenesis studies[9, 26]. Over the recent years, *Nes-gfp* has been shown to label not only neural stem cells but also a dynamic range of non-neural cell types in multiple organs, including heart[10, 12, 27]. It is therefore becoming clear that *Nes*-GFP+ expression, although restricted, should not be considered a definer of cell-lineage identity, but rather as a dynamic marker that is upregulated in specific scenarios by distinct cell types, including ECs, as we show here during cardiac development. In our study, we have employed these *Nestin*-related transgenic models just as a tool for visualizing developing coronary vessels. Of interest, several reports have found expression of the endogenous Nestin protein in rat and human blood vessels[28-30], particularly during neovascularization and following myocardial infarction[31]. It will be interesting to inspect further the biological relevance of the intermediate filament Nestin's cellular function in this context. According to the post-infarct temporal pattern of expression in adult heart, it has been suggested that Nestin may be needed for the cardiac reparative angiogenesis response[32]. Therefore, future studies will be required to assess whether Sox17 (or other SoxF factors) might play any role in regulating Nestin endogenous re-expression and, perhaps, participate in the vascular remodeling under pathological conditions.

The developmental origins of coronary vessels has remained a controversial topic in recent years, with the SV and the endocardium considered two of the main sources[2, 16, 17, 33, 34]. Despite the relative contributions of each compartment, it is increasingly clear that the developmental assembly of the coronary system is highly plastic, although still very poorly defined, with compensation of one source for deficiencies from the other to ultimate assure the proper functional vascularization of the heart, which is critical for the further growth and survival of the embryo[16]. An emerging concept in the vascular biology field is EC heterogeneity within vascular beds and organ-specific EC signatures. In this study, we performed RNA-seq profiling at high depth after precise separation of coronary and endocardial ECs at E13.5 and E17.5. An analogous separation was previously reported by Bin Zhou's lab using *Npr3-CreER* and *Fabp4-Cre* mouse lines, which allowed to prospectively fate-map and isolate endocardium and coronary vessels, respectively, from E14.5 hearts[33]. While our current expression datasets are consistent with those reported by Zhang *et al.* for the equivalent populations (not shown), our method allows to segregate and isolate these subpopulations from the very same pool of hearts, allowing for a better developmental synchronicity and better sample matching. Moreover, taken advantage of our strategy, we could perform a second RNAseq from the three segregated subsets of cardiac ECs (endocardium, intramyocardial arteries/capillaries and subepicardial veins) at E17.5. Single-cell (sc) transcriptomics has emerged as a potent technology to identify cellular heterogeneity, while bulk RNAseq can better capture subtle gene expression differences due to its higher sequencing depth. Indeed, our transcriptional profiling between prospective arteries and veins confirms and complements the recently reported scRNAseq analysis of cardiac cells building the coronary arteries by the Red-Horse lab[35].

In this work, we have identified putative binding motifs for Sox17/SoxF within the rat *Nestin* second intron sequence, most likely responsive for its coronary arteriogenic activation. In general, SOX family factors require other binding partners and co-factors, which are tissue-and cell-type specific, for achieving full transcriptional activation of target genes. Previous studies showed a synergistic inactivation between group B1/C SOX and class III POU to regulate *Nestin* enhancer in neural progenitors[36]. The SOX:POU motif is located in the CR2, no POU-family member gene expression was detected in our RNAseq data. It remains to be defined which other TFs may synergistically cooperate with Sox17 specifically in coronECs to regulate the neural enhancer, besides the endothelial-abundant ETS factors[37]. A recent study evaluated the signaling pathways operative in

developing mouse hearts using a collection of well-characterized vascular enhancers[38]. Intriguingly, they described a preference for SoxF/RBPJ regulatory pathways in sinus-venosus-derived arterial vessels. Although we have not evaluated the role of Notch/RBPG in our system, Sox17 has been reported to act upstream of Notch, and hence fine-tune Notch signaling during vessel sprouting. Whereas the Wnt/β-catenin signaling pathway has been reported to be a downstream target of Sox17 in postnatal vasculature of the retina, another potential pathway that might be targeted by Sox17, in the vascular context, is VEGF signaling (which is also linked to Notch induction). Moreover, we have observed that *in vitro* overexpression of Sox17 in MCEC led to the induction of *Cxcl12* expression in these cells (data not shown). Thus, this chemokine could be a potential target downstream Sox17 in the coronary vasculature, coinciding with data reported by Corada et al. in brain endothelial cells. However, further investigation should be performed in vivo to confirm this observation and whether it is direct. In further studies, it will be interesting to compare the transcriptional profiling from coronary vessels between WT and Sox17 mutants and examine candidate signaling pathways, including Notch, Wnt/β-catenin, VEFG, hypoxia (HIF factors) and Cxcl12-mediated signaling.

Initial confocal imaging and transcriptional profiling data suggested that Sox17 is not normally expressed in the ventricular endocardium. However, we observed that some cells at the trabecular base upregulate Sox17, invaginate, and penetrate into the compact myocardium (giving rise to endocardial flower-like structures). Interestingly, *Nes-gfp* reporter is also activated in these endocardial-derived sprouts that invade the ventricle. We speculate that Sox17 activation is required in sprouting coronary vessels, regardless of their origin (SV- or endocardium-derived vessels).

Next, we investigated the role of Sox17 in the formation of the coronary vessels by conditional deleting in coronECs with the *Nes-CreER* driver line. A similar goal was pursued by the Dejana lab to analyze the role of *Sox17* in controlling the brain-blood barrier permeability using an inducible *Cdh5-CreER^{T2}* driver to inactivate *Sox17* in ECs[39]. Considering that SoxF factors (including *Sox17*) play an important role in early endocardial formation and are required for heart development[40], we leveraged the *Nes-CreER* driver to restrict *Sox17* excision primarily to coronary vessels, thus preserving endocardial ECs, thus avoiding indirect effects from the endocardium. It has been suggested that endocardial–derived coronary vessels can expand and fully compensate for impaired vessel development in several mutants such as *Apj* or *Ccbe1*, which present defective development of SV-derived vascular plexus[16]. Intriguingly, the activated endocardium seems to upregulate *Sox17* (which is usually downregulated in these cells). In our work, we have also observed an increased expression of Sox17+ cells in the prospective ventricular activated endocardium. Therefore, we noticed the presence of residual Sox17+cells partially integrated into the defective arterioles, which are most likely derived from non-recombined cells of the activated endocardium. However, there was no full arterial remodeling of the primary plexus even under overexpression conditions. These results suggest that there is a critical threshold of Sox17+ pre-arterial ECs to populate the maturing coronary arteries, and correctly form the left CAs. It is known that remodeling of CAs requires of fluid shear stress signals triggered after attachment of coronary plexus to the aorta. While the phenotype observed could be related with this process, we found normal attachment to the aorta in our mutants. On the other hand, sub-epicardial coronary veins in the heart's dorsal surface remained unaffected in the absence of Sox17, suggesting that this TF may not be necessary for its correct remodeling.

In summary, we demonstrate that in coronary vessels, lack of *Sox17* cannot be compensated by overexpression of the other SoxF factors as described in other tissues. Even if the penetrance was variable in each littermate, most of the analyzed hearts showed lack of LCA in the ventral surface, whereas complete absence of RCA in the dorsal part of the heart was less common. The strongest phenotype showed absence of developing coronary plexus in the ventral surface of mutant hearts. These findings suggest that, in contrast to what happens in other gene mutants, the compensatory upregulation of Sox17 in activated endocardial cells is not enough to fully counteract the coronary vascular phenotype when this TF is not expressed in developing coronary vessels. Altogether, conditional deletion of coronECs during the initial sprouting phase (E10.5-E12.5) revealed the crucial role of Sox17 factor in the correct colonization of developing plexus in embryonic hearts as well as subsequent remodeling into mature arteries and arterioles.

ACKNOWLEDGMENTS

We want to thank P.M.C. laboratory members at CNIC and UPF for help and feedback. We are very grateful to Andrés Hidalgo and his team for support and critically reading the manuscript. We thank Diana Velázquez and Jorge Alegre's group at CNIC for help in protein purification and EMSAs; to Abel Sánchez-Aguilera and former S.M.F. lab members for help and critical discussions; the technical units of CNIC for help and assistance; Ana Ricote and Raquel Baeza for mouse husbandry; Dr. Stuart J. Pocock for statistical advice. The authors also thank Sean Morrison for sharing the Sox17-floxed line, which was kindly provided by Monica Corada and Elisabetta Dejana.

SOURCES OF FUNDING

This work was supported by grants from the Spanish *Ministerio de Economía y Competitividad* (BFU2012-35892 and *Ramón y Cajal* Program grant RYC-2011-09209 to J.I.), and FPIMINECO13 fellowship (BES-2013-065514) to S.G.H. Additionally, S.M.-F laboratory received funding from Plan Nacional grant SAF-2011-30308, Ramón y Cajal Program grant RYC-2009-04703, Spanish Cell Therapy Network TerCel, Marie Curie Career Integration Program grant FP7-PEOPLE-2011-RG-294096, ConSEPOC-Comunidad de Madrid grant S2010/BMD-2542 and Howard Hughes International Early Career Scientist grant. This study was also supported by Intramural grants from the Severo Ochoa program (IGP-SO), Fundació La Marató de TV3 (120/C/2015-20153032), and grant RTI2018-095497-B-I00 from MCIU to A.H.; and to MINECO RTI2018-096068, AFM, MDA, LaCaixa-HR17-00040, UPGRADE-H2020-825825 grants and ERC Advanced Grant-741538 to PMC. The CNIC is supported by the *Instituto de Salud Carlos III* (ISCIII), the *Ministerio de Ciencia e Innovación* (MCIN) and the Pro CNIC Foundation, and is a Severo Ochoa Center of Excellence (SEV-2015-0505). The UPF is a María de Maeztu Unit of Excellence (MDM-2014-0370).

DISCLOSURES

None.

SUPPLEMENTAL MATERIALS

Expanded Methods Section

Online Tables I – VII

Online Figures I – VIII

Data Set GSE147128

References[41-60]

REFERENCES

1. Red-Horse K, Ueno H, Weissman IL, Krasnow MA. Coronary arteries form by developmental reprogramming of venous cells. *Nature*. 2010;464:549-553
2. Tian X, Pu WT, Zhou B. Cellular origin and developmental program of coronary angiogenesis. *Circ Res*. 2015;116:515-530
3. Cavallero S, Shen H, Yi C, Lien C-L, Kumar SR, Sucov HM. Cxcl12 signaling is essential for maturation of the ventricular coronary endothelial plexus and establishment of functional coronary circulation. *Dev. Cell.* 2015;33:469-477
4. Pérez-Pomares J-M, de la Pompa JL, Franco D, Henderson D, Ho SY, Houyel L, Kelly RG, Sedmera D, Sheppard M, Sperling S, Thiene G, van den Hoff M, Basso C. Congenital coronary artery anomalies: A bridge from embryology to anatomy and pathophysiology--a position statement of the development, anatomy, and pathology esc working group. *Cardiovasc. Res.*2016;109:204-216
5. Zimmerman L, Parr B, Lendahl U, Cunningham M, McKay R, Gavin B, Mann J, Vassileva G, McMahon A. Independent regulatory elements in the nestin gene direct transgene expression to neural stem cells or muscle precursors. *Neuron*. 1994;12:11-24
6. Suzuki S, Namiki J, Shibata S, Mastuzaki Y, Okano H. The neural stem/progenitor cell marker nestin is expressed in proliferative endothelial cells, but not in mature vasculature. *J Histochem Cytochem* 2010;58:721-730
7. Lendahl U, Zimmerman LB, McKay RD. Cns stem cells express a new class of intermediate filament protein. *Cell*. 1990;60:585-595
8. Josephson R, Müller T, Pickel J, Okabe S, Reynolds K, Turner PA, Zimmer A, McKay RD. Pou transcription factors control expression of cns stem cell-specific genes. *Development (Cambridge)*. 1998;125:3087-3100
9. Mignone JL, Kukekov V, Chiang A-S, Steindler D, Enikolopov G. Neural stem and progenitor cells in nestin-gfp transgenic mice. *J. Comp. Neurol.* 2004;469:311-324
10. Amoh Y, Yang M, Li L, Reynoso J, Bouvet M, Moossa AR, Katsuoka K, Hoffman RM. Nestin-linked green fluorescent protein transgenic nude mouse for imaging human tumor angiogenesis. *Cancer Res*. 2005;65:5352-5357
11. Xu C, Gao X, Wei Q, Nakahara F, Zimmerman SE, Mar J, Frenette PS. Stem cell factor is selectively secreted by arterial endothelial cells in bone marrow. *Nat Commun.* 2018;9:2449
12. Méndez-Ferrer S, Michurina TV, Ferraro F, Mazloom AR, Macarthur BD, Lira SA, Scadden DT, Ma'ayan A, Enikolopov GN, Frenette PS. Mesenchymal and haematopoietic stem cells form a unique bone marrow niche. *Nature*. 2010;466:829-834
13. Isern J, García-García A, Martín AM, Arranz L, Martín-Pérez D, Torroja C, Sánchez-Cabo F, Méndez-Ferrer S. The neural crest is a source of mesenchymal stem cells with specialized hematopoietic stem cell niche function. *eLife*. 2014;3:e03696
14. Das S, Goldstone AB, Wang H, Farry J, D'Amato G, Paulsen MJ, Eskandari A, Hironaka CE, Phansalkar R, Sharma B, Rhee S, Shamskhou EA, Agalliu D, de Jesus Perez V, Woo YJ, Red-Horse K. A unique collateral artery development program promotes neonatal heart regeneration. *Cell*. 2019;176:1128-1142.e1118
15. Ivins S, Chappell J, Vernay B, Suntharalingham J, Martineau A, Mohun TJ, Scambler PJ. The cxcl12/cxcr4 axis plays a critical role in coronary artery development. *Dev Cell.* 2015;33:455-468
16. Sharma B, Ho L, Ford GH, Chen HI, Goldstone AB, Woo YJ, Quertermous T, Reversade B, Red-Horse K. Alternative progenitor cells compensate to rebuild the coronary vasculature in elabela- and apj-deficient hearts. *Dev Cell.* 2017;42:655-666.e653
17. Wu B, Zhang Z, Lui W, Chen X, Wang Y, Chamberlain AA, Moreno-Rodriguez RA, Markwald RR, O'Rourke BP, Sharp DJ, Zheng D, Lenz J, Baldwin HS, Chang C-P, Zhou B. Endocardial cells form the coronary arteries by angiogenesis through myocardial-endocardial vegf signaling. *Cell*. 2012;151:1083-1096
18. Tian X, Hu T, Zhang H, He L, Huang X, Liu Q, Yu W, He L, Yang Z, Zhang Z, Zhong TP, Yang X, Yang Z, Yan Y, Baldini A, Sun Y, Lu J, Schwartz RJ, Evans SM, Gittenberger-De Groot AC, Red-Horse K, Zhou B. Subepicardial endothelial cells invade the embryonic ventricle wall to form coronary arteries. *Cell Res.* 2013;23:1075-1090

19. Balordi F, Fishell G. Mosaic removal of hedgehog signaling in the adult svz reveals that the residual wild-type stem cells have a limited capacity for self-renewal. *J Neurosci.* 2007;27:14248-14259
20. Chen KG, Johnson KR, Robey PG. Mouse genetic analysis of bone marrow stem cell niches: Technological pitfalls, challenges, and translational considerations. *Stem cell rep*. 2017;9:1343-1358
21. Francois M, Koopman P, Beltrame M. Soxf genes: Key players in the development of the cardio-vascular system. *Int J Biochem Cell biol.* 2010;42:445-448
22. Corada M, Orsenigo F, Morini MF, Pitulescu ME, Bhat G, Nyqvist D, Breviario F, Conti V, Briot A, Iruela-Arispe ML, Adams RH, Dejana E. Sox17 is indispensable for acquisition and maintenance of arterial identity. *Nat Commun.* 2013;4:2609
23. Miquerol L, Thireaau J, Bideaux P, Sturny R, Richard S, Kelly RG. Endothelial plasticity drives arterial remodeling within the endocardium after myocardial infarction. *Circ Res*. 2015;116(11):1765-71
24. Downes M, Francois M, Ferguson C, Parton RG, Koopman P. Vascular defects in a mouse model of hypotrichosis-lymphedema-telangiectasia syndrome indicate a role for sox18 in blood vessel maturation. *Hum. Mol. Genet.* 2009;18:2839-2850
25. Zhou Y, Williams J, Smallwood PM, Nathans J. Sox7, sox17, and sox18 cooperatively regulate vascular development in the mouse retina. *PLoS ONE*. 2015;10:e0143650-0143622
26. Kawaguchi A, Miyata T, Sawamoto K, Takashita N, Murayama A, Akamatsu W, Ogawa M, Okabe M, Tano Y, Goldman SA, Okano H. Nestin-egfp transgenic mice: Visualization of the self-renewal and multipotency of cns stem cells. *Mol Cell Neurosci.* 2001;17:259-273
27. El-Helou V, Chabot A, Gosselin H, Villeneuve L, Clavet-Lanthier M-E, Tanguay J-F, Enikolopov G, Fernandes KJL, Jasmin J-F, Calderone A. Cardiac resident nestin (+) cells participate in reparative vascularisation. *J Cell Physiol.* 2013;228:1844-1853
28. Mokrý J, Nemecek J. Angiogenesis of Extra- And Intraembryonic Blood Vessels Is Associated With Expression of Nestin in Endothelial Cells. Folia Biol (Praha). 1998;44(5)155-61
29. Mokrý J, Ehrmann J, Karbanová J, Cízková D, Soukup T, Suchánek J, Filip S, Kolár Z. Expression of Intermediate Filament Nestin in Blood Vessels of Neural and Non-Neural Tissues. Acta Medica (Hradec Kralove). 2008;51(3):173-9
30. Dusart P, Fagerberg L, Perisic L, Civelek M, Struck E, Hedin U, Uhlén M, Trégouët DA, Renné T, Odeberg J, M Butler LM. A Systems-Approach Reveals Human Nestin Is an Endothelial-Enriched, Angiogenesis-Independent Intermediate Filament Protein. Sci Rep. 2018;8(1):14668
31. Mokry J, Pudil R, Ehrmann J, Cizkova D, Osterreicher J, Filip S, Kolar Z. Re-expression of Nestin in the Myocardium of Postinfarcted Patients. Virchows Archiv. 2008;453(1):33-41
32. Calderone A. The Biological Role of Nestin (+)-Cells in Physiological and Pathological Cardiovascular Remodeling. Front Cell Dev Biol. 2018;14;6:15
33. Zhang H, Pu W, Li G, Huang X, He L, Tian X, Liu Q, Zhang L, Wu SM, Sucov HM, Zhou B. Endocardium minimally contributes to coronary endothelium in the embryonic ventricular free walls. *Circ Res.* 2016;118:1880-1893
34. Tian X, Hu T, Zhang H, He L, Huang X, Liu Q, Yu W, He L, Yang Z, Yan Y, Yang X, Zhong TP, Pu WT, Zhou B. Vessel formation. De novo formation of a distinct coronary vascular population in neonatal heart. Science. 2014;345(6192):90-4
35. Su T, Stanley G, Sinha R, D'Amato G, Das S, Rhee S, Chang AH, Poduri A, Raftrey B, Dinh TT, Roper WA, Li G, Quinn KE, Caron KM, Wu S, Miquerol L, Butcher EC, Weissman I, Quake S, Red-Horse K. Single-cell analysis of early progenitor cells that build coronary arteries. *Nature*. 2018;559:356-362
36. Tanaka S, Kamachi Y, Tanouchi A, Hamada H, Jing N, Kondoh H. Interplay of sox and pou factors in regulation of the nestin gene in neural primordial cells. *Mol Cell Biol.* 2004;24:8834-8846
37. Wythe JD, Dang LTH, Devine WP, Boudreau E, Artap ST, He D, Schachterle W, Stainier DYR, Oettgen P, Black BL, Bruneau BG, Fish JE. Ets factors regulate vegf-dependent arterial specification. *Dev Cell.* 2013;26:45-58

38. Payne S, Gunadasa-Rohling M, Neal A, Redpath AN, Patel J, Chouliaras KM, Ratnayaka I, Smart N, De Val S. Regulatory pathways governing murine coronary vessel formation are dysregulated in the injured adult heart. Nat Commun. 2019;10(1):3276
39. Corada M, Orsenigo F, Bhat GP, Conze LL, Breviario F, Cunha SI, Claesson-Welsh L, Beznoussenko GV, Mironov AA, Bacigaluppi M, Martino G, Pitulescu ME, Adams RH, Magnusson P, Dejana E. Fine-tuning of sox17 and canonical wnt coordinates the permeability properties of the blood-brain barrier. *Circ Res*. 2019;124:511-525
40. Saba R, Kitajima K, Rainbow L, Engert S, Uemura M, Ishida H, Kokkinopoulos I, Shintani Y, Miyagawa S, Kanai Y, Kanai-Azuma M, Koopman P, Meno C, Kenny J, Lickert H, Saga Y, Suzuki K, Sawa Y, Yashiro K. Endocardium differentiation through sox17 expression in endocardium precursor cells regulates heart development in mice. *Sci Rep.* 2019:1-11
41. Madisen L, Zwingman TA, Sunkin SM, Oh SW, Zariwala HA, Gu H, Ng LL, Palmiter RD, Hawrylycz MJ, Jones AR, Lein ES, Zeng H. A robust and high-throughput Cre reporting and characterization system for the whole mouse brain. *Nat Neurosci.* 2010;13(1):133-40
42. Kim I, Saunders TL, Morrison SJ. Sox17 dependence distinguishes the transcriptional regulation of fetal from adult hematopoietic stem cells. *Cell* 2007. 130:470–483.
43. Kisanuki YY, Hammer RE, Miyazaki J, Williams SC, Richardson JA, Yanagisawa M. Tie2-Cre transgenic mice: a new model for endothelial cell-lineage analysis in vivo. *Dev Biol.* 2001;230(2):230-42
44. Tzeng YS, Li H, Kang YL, Chen WC, Cheng WC, Lai DM. Loss of Cxcl12/Sdf-1 in adult mice decreases the quiescent state of hematopoietic stem/progenitor cells and alters the pattern of hematopoietic regeneration after myelosuppression. *Blood*. 2011;117(2):429-39
45. Hayashi S, Tenzen T, McMahon AP. Maternal inheritance of Cre activity in a Sox2Cre deleter strain. *Genesis*. 2003;37(2):51-3
46. Susaki EA, Tainaka K, Perrin D, Kishino F, Tawara T, Watanabe TM, Yokoyama C, Onoe H, Eguchi M, Yamaguchi S, Abe T, Kiyonari H, Shimizu Y, Miyawaki A, Yokota H, Ueda HR. Whole-brain imaging with single-cell resolution using chemical cocktails and computational analysis. *Cell*. 2014;157(3):726-39
47. Susaki EA, Tainaka K, Perrin D, Yukinaga H, Kuno A, Ueda HR. Advanced CUBIC protocols for whole-brain and whole-body clearing and imaging. *Nat Protoc.* 2015;10(11):1709-27
48. Kolesová H, Čapek M, Radochová B, Janáček J, Sedmera D. Comparison of different tissue clearing methods and 3D imaging techniques for visualization of GFP-expressing mouse embryos and embryonic hearts. *Histochem Cell Biol.*. 2016;146(2):141-52
49. Andrews S. FastQC: a quality control tool for high throughput sequence data. 2010. Available online at: http://www.bioinformatics.babraham.ac.uk/projects/fastqc
50. Martin, M. Cutadapt removes adapter sequences from high-throughput sequencing reads. *EMBnet J*. 2011;17:10
51. FASTX-Toolkit: http://hannonlab.cshl.edu/fastx_toolkit.
52. Li B, Dewey CN. RSEM: accurate transcript quantification from RNA-Seq data with or without a reference genome. *BMC Bioinformatics.* 2011;12:323–16
53. Ritchie ME, Phipson B, Wu D, Hu Y, Law CW, Shi W, Smyth GK. limma powers differential expression analyses for RNA-sequencing and microarray studies. *Nucleic Acids Res.* 2015. 43(7):e47
54. Sturn A, Quackenbush J, Trajanoski Z. Genesis: cluster analysis of microarray data. *Bioinformatics*. 2002.18;207–208
55. Huang DW, Sherman BT, Lempicki RA. Systematic and integrative analysis of large gene lists using DAVID bioinformatics resources. *Nat Protoc.* 2009. 4; 44–57
56. Yu G, Wang LG, Han Y, He QY. ClusterProfiler: an R package for comparing biological themes among gene clusters. *OMICS*. 2012. 16:284–287
57. Walter W, Sánchez-Cabo F, Ricote M. GOplot: an R package for visually combining expression data with functional analysis. *Bioinformatics*. 2015. 31;2912–2914
58. Barbieri SS, Weksler BB. Tobacco smoke cooperates with interleukin-1beta to alter beta-catenin trafficking in vascular endothelium resulting in increased permeability and induction of cyclooxygenase-2 expression in vitro and in vivo. *FASEB J.* 2007;21(8):1831-43

59. Mancini C, Messana E, Turco E, Brussino A, Brusco, A. Gene-targeted embryonic stem cells: real-time PCR assay for estimation of the number of neomycin selection cassettes. *Biol Proced Online.* 2011;13:10–4
60. Smith, MF, Delbary-Gossart, S. Electrophoretic Mobility Shift Assay (EMSA). *Methods Mol Med*. 2001;50:249–257

FIGURE LEGENDS

Figure 1. Temporal development of coronary plexus formation and arterial remodeling directly visualized by *Nes-gfp* allele expression.
(**A**) Representative image of a E12.5 *Nes-gfp; Tie2-Cre; R26-tomato* heart showing the overlay of the GFP and Tie2-lineage (tom) channels. (**A1**) Individual channels of an optical slice close to the dorsal surface. Inset from the boxed region shows an enlarged view of the sprouting GFP+ vessels. (**B-C**) Representative whole-mount confocal images of embryonic *Nes-gfp* clarified hearts, from E12.5 to P1 in the ventral and dorsal view, respectively. Arrowheads show remodeling zones of the prospective coronary arteries. (**D**) Representative confocal images from CUBIC-cleared hearts of *Nes-gfp; R26-Tomato (LSL-out)* at E13.5. Sprouts GFP+ emerging from the blood island located in the ventral surface of the heart. (E) A zoomed area from the RV is shown. Subepicardial GFP+ vessels (white arrowheads) have lower GFP levels than the intramyocardial plexus. Scale bar 300 μm and 100 μm in boxed areas.
RA, *right atrium*; *LA*, *left atrium*; *RV*, *right ventricle*; *LV*, *left ventricle*; *VG*, *ventricular groove*; *IVS*, *interventricular septum*; *SV*, *sinus venosus*.
z1:n designates the number of individual optical slices composing each projected stack.

Figure 2. Combination of *Nes-gfp* reporter and endomucin marker to differentiate ventricular endocardium from coronECs and also arteries from veins.
(**A**) FACS strategy to isolate ventricular endocardium from coronECs in enzymatically dissociated hearts. (**B**) Relative mRNA expression heatmap of selected endocardial-enriched (*Emcn*, *Npr3*) and coronary-enriched genes (*Apln*, *Fabp4*), assessed by quantitative reverse-transcription (qPCR) analysis of the indicated populations. Data are the average value of the individual replicate measurements (2-3), from two independent biological samples (each from >8 embryonic hearts pooled together). (**C**) Representative FACS plots showing the proportion between endocardium and coronary vessels throughout development. (**D**) CVs progressively downregulate GFP reporter and increase endomucin marker whereas CAs express high level of GFP and are negative for endomucin. (**E**) Immunostaining for Emcn on E17.5 heart sections and (F) Representative image of the whole-mount ventral view of E18.5 *Nes-gfp* heart showing that GFP reporter is downregulated in CVs and highly expressed in intramyocardial arteries and capillaries. Scale bars 500 μm in E and F (20 μm boxed areas); 500 μm in F (200 μm boxed areas).
Ao, *aorta*; *CA*, *coronary artery*; *CV*, *coronary vein*.

Figure 3. Characterization of *Nes-CreER*-derived lineage in the developing heart.
(**A**) Representative image of the dorsal whole-mount view of a E12.5 *Nes-CreER^{T2};R26-tomato* heart pulse-labeled with tamoxifen at E10.5 stage. (**B**) Boxed area show developing endothelial plexus traced in tomato (tom). (**C**) Scheme comparing tom+ traced cells at E17.5 when induced at E12.5 or E15.5, respectively. (**D**) Representative FACS analysis reveal that induction at E12.5 traced endothelial (>70%) and non-endothelial cells. Focus on endothelial subpopulation (Tom+ CD31+), we traced both arteries (Emcn-) and veins (Emcn+). (**E**) Induction at E15.5 trace almost exclusively coronECs (> 90%), restricted mainly into arteries (Emcn-). (**F**) Immunostaining confirm that induction at E12.5 trace all coronECs but not endocardium. (**G**) Tamoxifen at E15.5 exclusively trace intramyocardial arteries/capillaries. Scale bars 300 μm; 100 μm boxed areas.

Figure 4. Transcriptional profiling comparing ventricular endocardium versus coronary plexus ECs during sprouting (E13.5) and after remodeling phase (E17.5).
(**A-B**) Clustering of differentially expressed genes. 4,615 genes detected as differentially expressed with adj.*p*_value<0,05 and abs(logFC)>1 in the four contrasts represented in Online Figure VD, were grouped into 16 clusters using Kmeans on their expression profiles. Eleven of those preliminary clusters were selected and merged, to define five final clusters (I-V). (**A**) Heatmap showing relative expression levels of all genes in each final cluster, with indication of some representative gene. (**B**) Expression profiles of all genes in each final cluster, and mean expression profiles (dotted lines). (**C**) Circular GOplot representing a selection of enriched Gene Ontology terms detected for cluster II

genes, connected to the associated differentially expressed genes, as described in Methods. (**D**) Expression profile-based clustering of samples by PCA. (**E**) Detailed comparison of expression levels for selected candidate genes from cluster II. Data are mean ±SEM, from n=2-4 biological replicates (sorted from pooled 16-24 embryonic hearts for endocardium and coronary plexus at E13.5, and from 7-8 at E17.5, per each biological replicate). Adjusted *p*-values (Benjamini and Hochberg method) are shown.

Figure 5. Transcriptional profiling between ventricular endocardium, intramyocardial arteries/capillaries and subepicardial veins in E17.5 hearts.
(**A**) Expression profile-based clustering of samples by PCA. (**B**) GOplot representing a selection of enriched Gene Ontology associated to genes detected as differentially expressed (adj.p<0.05) in a contrast comparing arterial-enriched ECs and venous-enriched ECs. (**C**) and (**D**) Detailed comparison of expression levels for selected candidate genes in arterial-enriched ECs and venous-enriched ECs, respectively. Data are mean ±SEM, from n=3 biological replicates (each biological replicate from pools of 3 hearts for endocardium, and from pools of 4-5 hearts for arterial/venous-enriched samples, respectively). Adjusted *p*-values (Benjamini and Hochberg method) are shown, unless indicated. (**E**) Volcano plot summarizing differential expression analysis results (colored dots represent diferentially expressed genes with adj.$p\leq0.05$), for a comparison between endocardium (purple) and intramyocardial vessel (coronary plexus, red) transcriptomic profiles. Selected endocardial- and arterial-enriched specific genes are featured.

Figure 6. Dynamic expression of *Sox17* in developing coronary endothelial cells.
(**A**) Heatmap shows SoxF gene expression in endocardium and coronary plexus at E13.5 and E17.5, respectively. (**B**) mRNA expression of *Egfp* and *Sox17* in each sorted sub-populations. Data are mean ±SEM from n=2-4 biological replicates, as in figure panels 4E and 5C-D. Adjusted *p*-values (Benjamini and Hochberg method) are shown, unless indicated. (**C**) Sagittal sections in E11.5 *Nes-gfp*+ hearts showing *Sox17*-expressing cells in emerging coronary plexus and its colocalization with emcn and GFP. (**D**) Sagittal sections of E14.5 hearts showing downregulation of *Sox17* expression in subepicardial ECs as well as *Nes-gfp* reporter. (**E**) Quantification of the maximum fluorescence intensity (MFI) of Sox17 marker and *Nes-gfp* expression in subepicardial and intramyocardial ECs in E13.5 heart sections. Data (measured from n=5 ventricular sections, with >35 cells quantified per each individual region/image), are presented as violin plots; the solid horizontal line indicates the median. Statistical significance assessed by the Mann-Whitney U-test. (**F**) Representative image of the whole-mount of E17.5 *Nes-gfp*+ heart shows Sox17 expression restricted to CAs after remodeling (boxed area). Scale bar 300 μm and 100 μm in boxed areas.
AVC, atrioventricular canal; OFT, outflow tract.

Figure 7. Interaction of *Sox17* transcription factor with *Nestin* neural enhancer *in vitro.*
(**A**) Multispecies alignment using ClustalW shows that *Nes* second intron enhancer contains two putative binding sites for SOX TFs (CR1 and CR2, respectively), as well as other binding sites for ETS and POU factors. (**B**) EMSA assay demonstrates that *Sox17* is able to physically interact *in vitro* with both CR1 (lanes 2-4) and CR2 (lanes 5-7), showing specificity for CR1 where the protein was competed by excess unlabeled self-probe (WT, lanes 3) but not by mutant self-probe (MUT, lane 4). (**C**) Luciferase assay in MCEC cells overexpressing Sox17 or Sox18, respectively. (**D**)Tube formation assay in HUVECs transfected with a control plasmid and *Sox18 Ragged Opossum*-expressing plasmid (*RaOp*, right panel) shows that overexpression of the dominant negative protein in ECs abolish the tube formation. (**E**) Quantification of total number of loops and branching points comparing control and mutant conditions. Data are mean ±SEM; n=3 (C and D); *p*-values were determined by 1-way ANOVA with Tukey correction (C) and the unpaired *t*-test (E).

Figure 8. Sox17 is required for the correct formation of developing vessels and posterior remodeling of coronary arteries.
(A) Scheme of tamoxifen inductions at E10.5 and E12.5 and analysis of E16.5 hearts. (**B**) Whole-mount of *Nes-gfp*+ hearts show that $Sox17^{cKO}$ have impaired development of coronary plexus and

completely abolished the remodeling of CAs (right panel, asterisk) compared with control hearts (left panel, arrowheads). (**C**) Ventral and (**D**) dorsal view of tom+ hearts showing Tom+ ECs where Sox17 is abolish in cKO hearts. Boxed areas show normal remodeling of the CAs in WT hearts (C1, LCA in ventral surface; D1, right CA in dorsal surface). In mutant hearts, cells that express Sox17 are insufficient for normal remodeling boxed area C2 and D3). Scale bars, 500 μm; 100 μm in boxed areas. The most representative images better depicting the observed phenotypes are shown.

NOVELTY and SIGNIFICANCE

What is known?

- Tissue-specific sets of regulatory sequences, known as enhancers, dynamically regulate gene expression during mammalian organogenesis.
- Previous genetic tools have been applied to study the coronary and endocardial lineages. However, the precise pathways that regulate coronary angiogenesis are not completely defined at the molecular level.
- Coronary arteriogenesis involves the remodeling of an immature vascular plexus. This primitive network of small vessels undergoes an extensive morphogenic process, transforming into mature, large-caliber arteries.

What new information does this article contribute?

- This study provides a thorough characterization of the *Nes-gfp* and *Nes-creERT2* transgenic mouse lines for studying the emergence of coronary vessels
- They have examined a previously reported neural regulatory region within *Nestin*'s gene and found that it is active in developing coronary vessels.
- *Nestin*'s enhancer activity is specific to coronary vessels regardless of their possible origins (sinus venosus or endocardium), but it barely active in the endocardial layer of the developing four-chambered heart.
- The enhancer drives gene expression in sprouting coronary endothelial cells and contains putative binding motifs for the Sox17 transcriptional factor, that could be required for its arterial activity.
- Sox17 is a critical regulator of arterial formation during coronary development. The remodeling of prospective arterial coronary vasculature is profoundly impaired by Sox17 genetic loss of function in the developing heart.

Coronary artery disease is the main leading cause of cardiovascular-related deaths worldwide. Current research in vascular regenerative medicine could benefit from a better knowledge of how coronary arteries form during development, or how these pathways might become reactivated during disease. In mammals, the coronary endothelium and their mural layer are assembled from multiple cellular progenitor sources, controlled by distinct regulatory mechanisms.

Here, we show that the previously generated *Nes-gfp* and *Nes-CreER*^{T2} mouse lines, based on the presence of a neural regulatory element from the *Nestin's* gene, are additional tools for precisely studying the development of the coronary vasculature and the arteriogenic differentiation. We found that the transcription factor Sox17 is progressively enriched in intramyocardial vessels and prospective coronary arteries. Several binding sites were identified within the *Nestin's* enhancer region, suggesting that Sox17 could be needed for its arterial activity. Furthermore, coronary-specific loss of *Sox17* leads to defective arterial remodeling of the coronary plexus, establishing a potential new future therapeutic pathway to target for cardiac vascular regeneration.

Figure 1

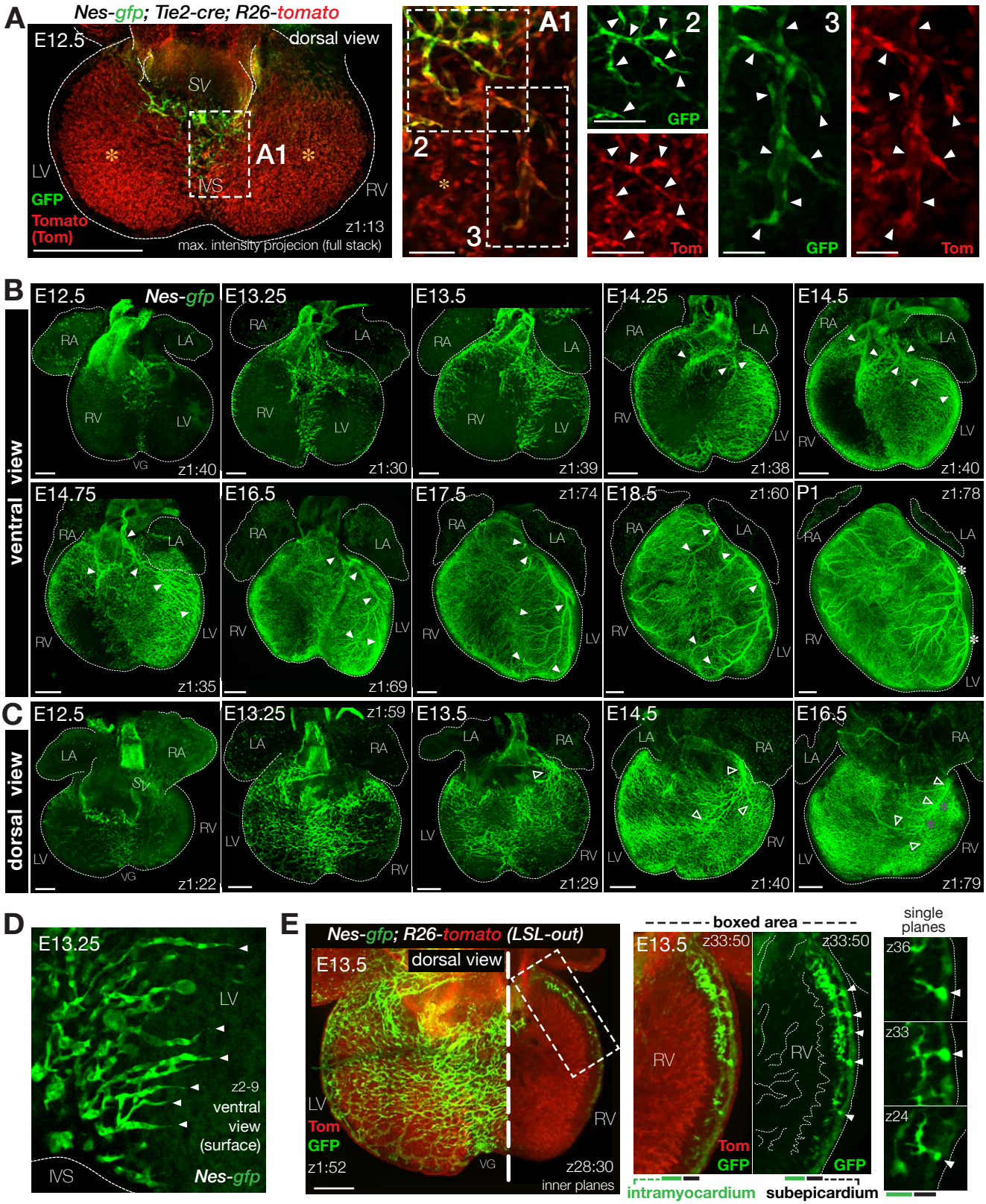
A
Nes-gfp; Tie2-cre; R26-tomato
E12.5
dorsal view
SV
A1
LV
IVS
RV
GFP
Tomato (Tom)
z1:13
max. intensity projecion (full stack)
A1
2
3
GFP
Tom
3
GFP
Tom
B
ventral view
E12.5
Nes-gfp
E13.25
E13.5
E14.25
E14.5
RA
LA
RV
LV
VG
z1:40
z1:30
z1:39
z1:38
z1:40
E14.75
E16.5
E17.5
z1:74
E18.5
z1:60
P1
z1:78
z1:35
z1:69
C
dorsal view
E12.5
E13.25
z1:59
E13.5
E14.5
E16.5
SV
z1:22
z1:29
z1:40
z1:79
D
E13.25
LV
z2-9
ventral view (surface)
IVS
Nes-gfp
E
Nes-gfp; R26-tomato (LSL-out)
E13.5
dorsal view
LV
Tom
GFP
RV
z1:52
VG
z28:30
inner planes
boxed area
E13.5
z33:50
z33:50
RV
Tom
GFP
GFP
intramyocardium
subepicardium
single planes
z36
z33
z24

Figure 2

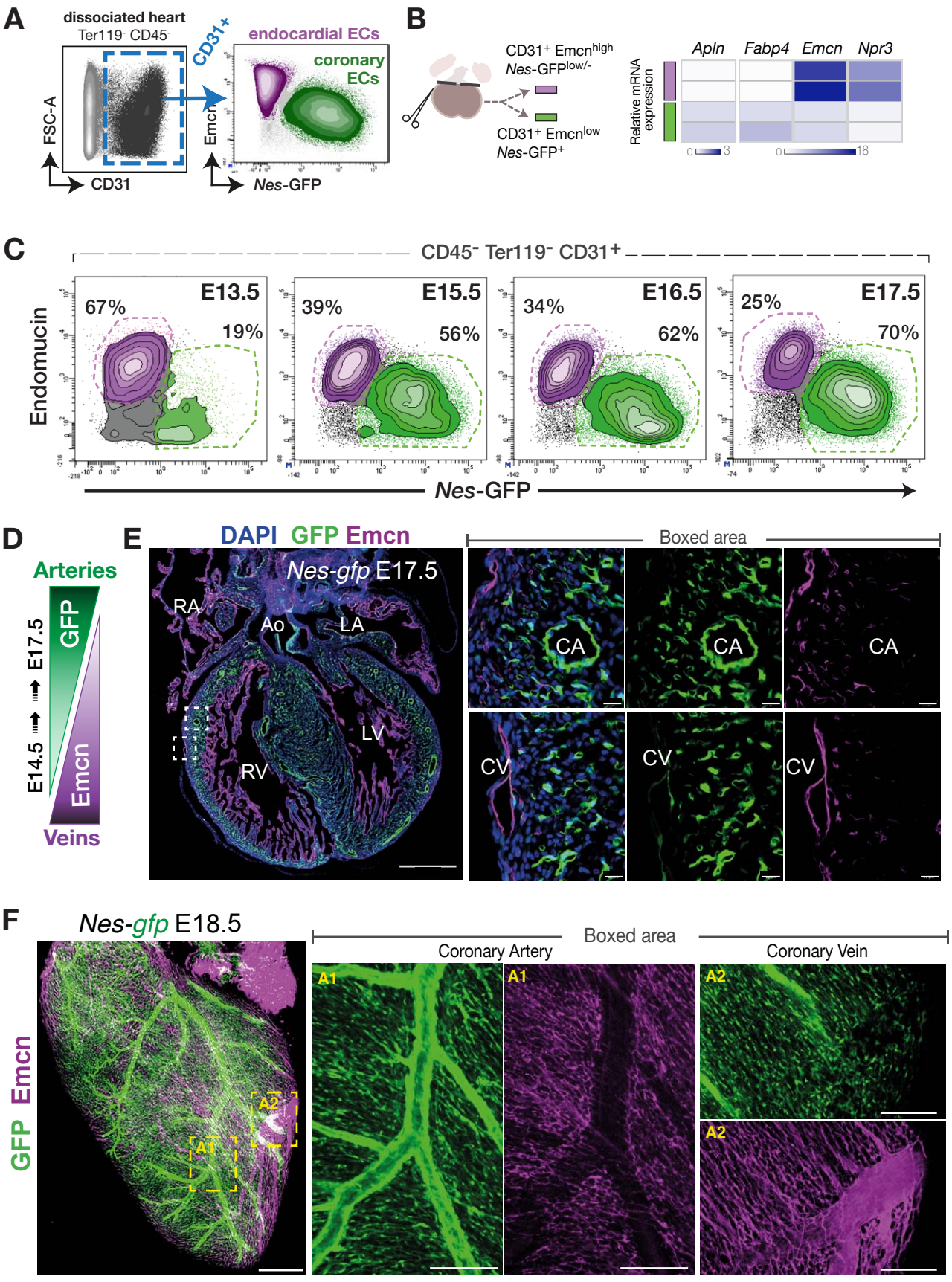
A
dissociated heart
Ter119- CD45-
CD31+
endocardial ECs
coronary ECs
FSC-A
CD31
Emcn
Nes-GFP
B
CD31+ Emcnhigh
Nes-GFPlow/-
CD31+ Emcnlow
Nes-GFP+
Apln
Fabp4
Emcn
Npr3
Relative mRNA expression
0
3
0
18
C
CD45- Ter119- CD31+
Endomucin
E13.5
67%
19%
E15.5
39%
56%
E16.5
34%
62%
E17.5
25%
70%
Nes-GFP
D
Arteries
GFP
E17.5
E14.5
Emcn
Veins
E
DAPI GFP Emcn
Nes-gfp E17.5
RA
Ao
LA
LV
RV
Boxed area
CA
CV
F
Nes-gfp E18.5
GFP Emcn
A1
A2
Boxed area
Coronary Artery
Coronary Vein

Figure 3

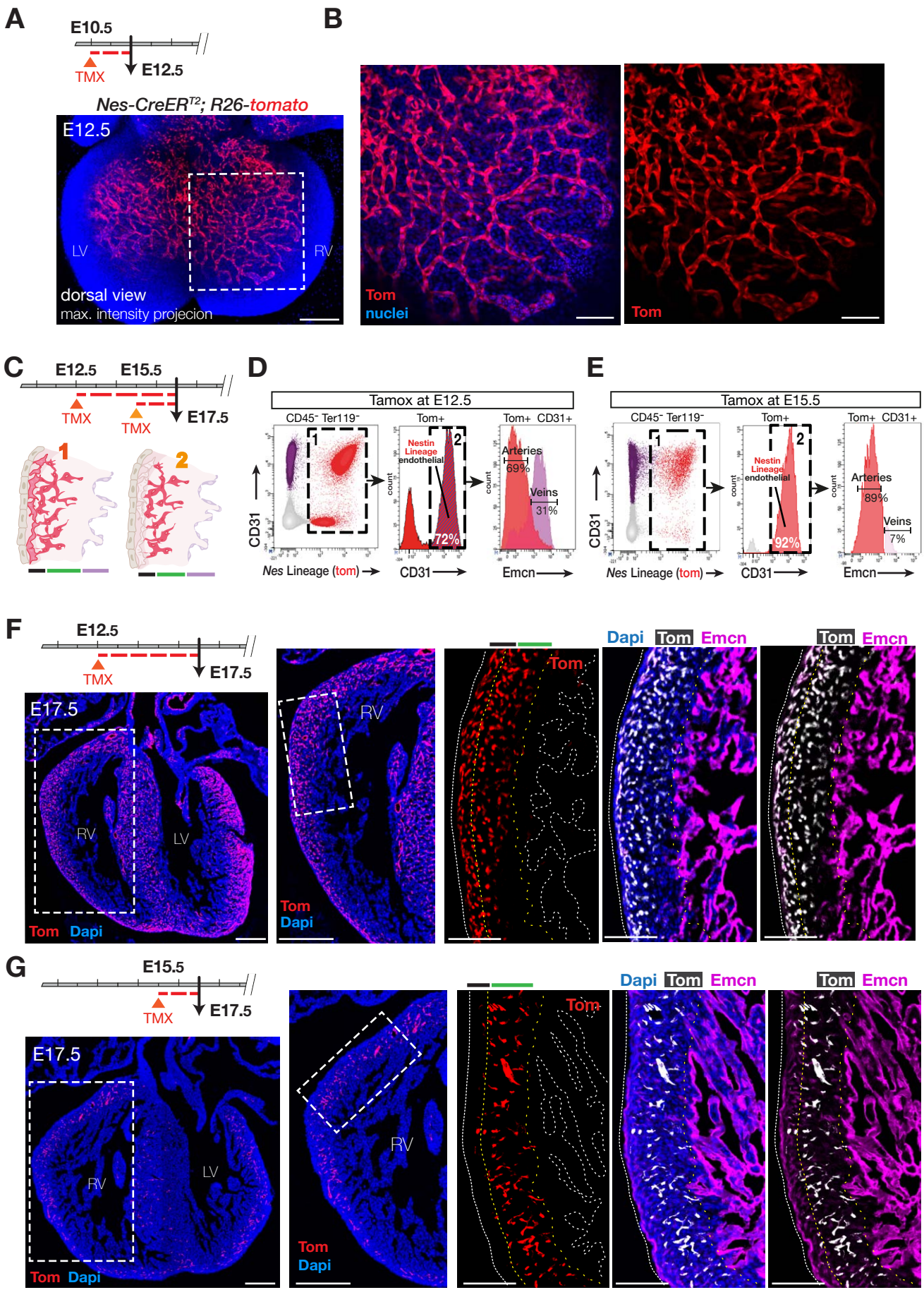
A
E10.5
E12.5
TMX
Nes-CreER^{T2}; R26-tomato
E12.5
LV
RV
dorsal view
max. intensity projecion
B
Tom
nuclei
Tom
C
E12.5
E15.5
E17.5
TMX
TMX
1
2
D
Tamox at E12.5
CD45$^-$ Ter119$^-$
Tom+
Tom+ CD31+
1
2
Nestin Lineage endothelial
72%
Arteries
69%
Veins
31%
CD31
count
Nes Lineage (tom)
CD31
Emcn
E
Tamox at E15.5
CD45$^-$ Ter119$^-$
Tom+
Tom+ CD31+
1
2
Nestin Lineage endothelial
92%
Arteries
89%
Veins
7%
CD31
count
Nes Lineage (tom)
CD31
Emcn
F
E12.5
E17.5
TMX
E17.5
RV
LV
Tom Dapi
RV
Tom
Dapi
Tom
Dapi Tom Emcn
Tom Emcn
G
E15.5
E17.5
TMX
E17.5
RV
LV
Tom Dapi
RV
Tom
Dapi
Tom
Dapi Tom Emcn
Tom Emcn

Figure 4

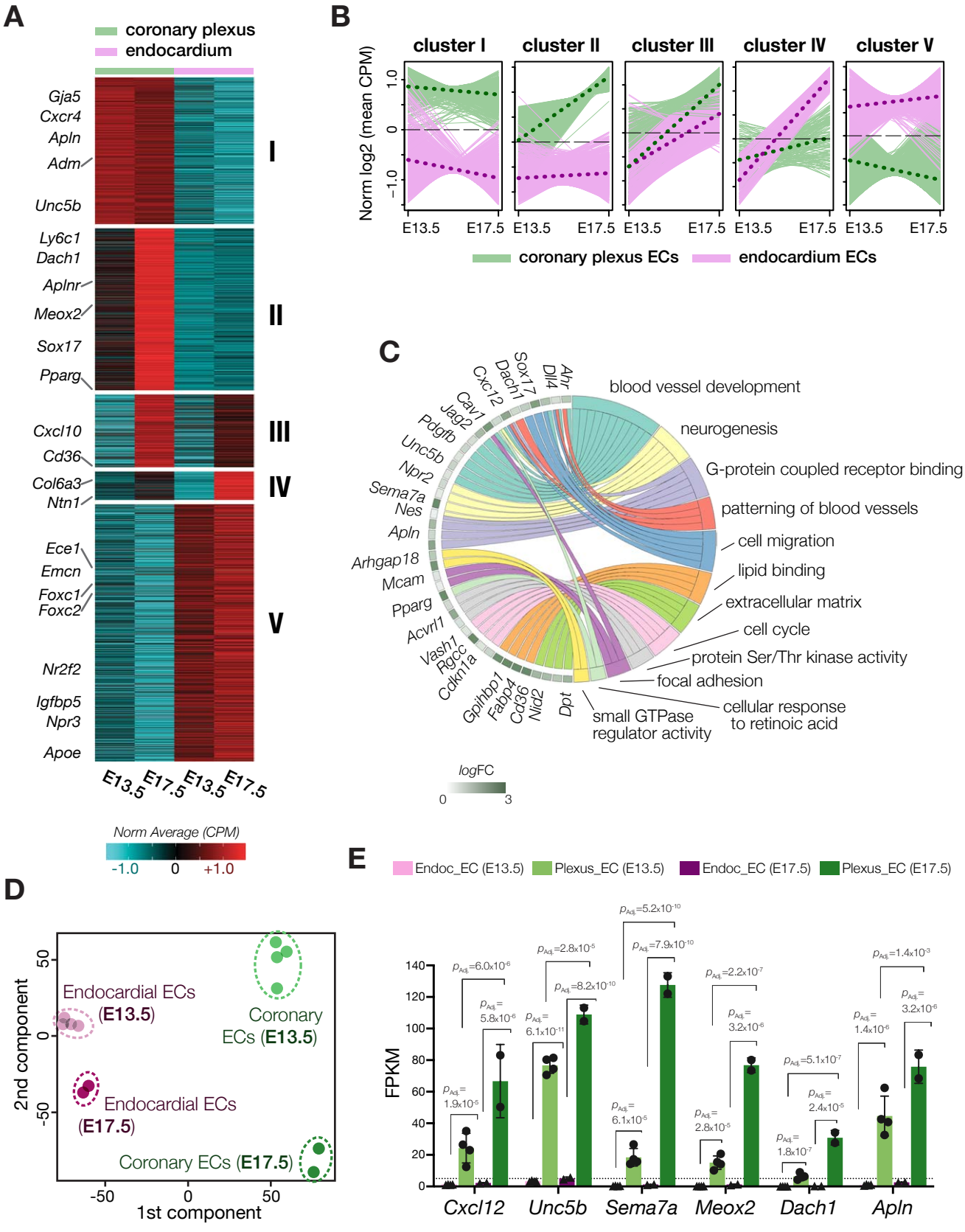
A
coronary plexus
endocardium
Gja5
Cxcr4
Apln
Adm
Unc5b
Ly6c1
Dach1
Aplnr
Meox2
Sox17
Pparg
Cxcl10
Cd36
Col6a3
Ntn1
Ece1
Emcn
Foxc1
Foxc2
Nr2f2
Igfbp5
Npr3
Apoe
I
II
III
IV
V
E13.5
E17.5
E13.5
E17.5
Norm Average (CPM)
-1.0
0
+1.0
B
cluster I
cluster II
cluster III
cluster IV
cluster V
Norm log2 (mean CPM)
1.0
0
−1.0
E13.5
E17.5
coronary plexus ECs
endocardium ECs
C
Ahr
Dll4
Sox17
Dach1
Cxc12
Cav1
Jag2
Pdgfb
Unc5b
Npr2
Sema7a
Nes
Apln
Arhgap18
Mcam
Pparg
Acvrl1
Vash1
Rgcc
Cdkn1a
Gpihbp1
Fabp4
Cd36
Nid2
Dpt
blood vessel development
neurogenesis
G-protein coupled receptor binding
patterning of blood vessels
cell migration
lipid binding
extracellular matrix
cell cycle
protein Ser/Thr kinase activity
focal adhesion
cellular response to retinoic acid
small GTPase regulator activity
logFC
0
3
D
2nd component
50
0
-50
Endocardial ECs (E13.5)
Coronary ECs (E13.5)
Endocardial ECs (E17.5)
Coronary ECs (E17.5)
-50
0
50
1st component
E
Endoc_EC (E13.5)
Plexus_EC (E13.5)
Endoc_EC (E17.5)
Plexus_EC (E17.5)
FPKM
140
120
100
80
60
40
20
0
Cxcl12
Unc5b
Sema7a
Meox2
Dach1
Apln

Figure 5

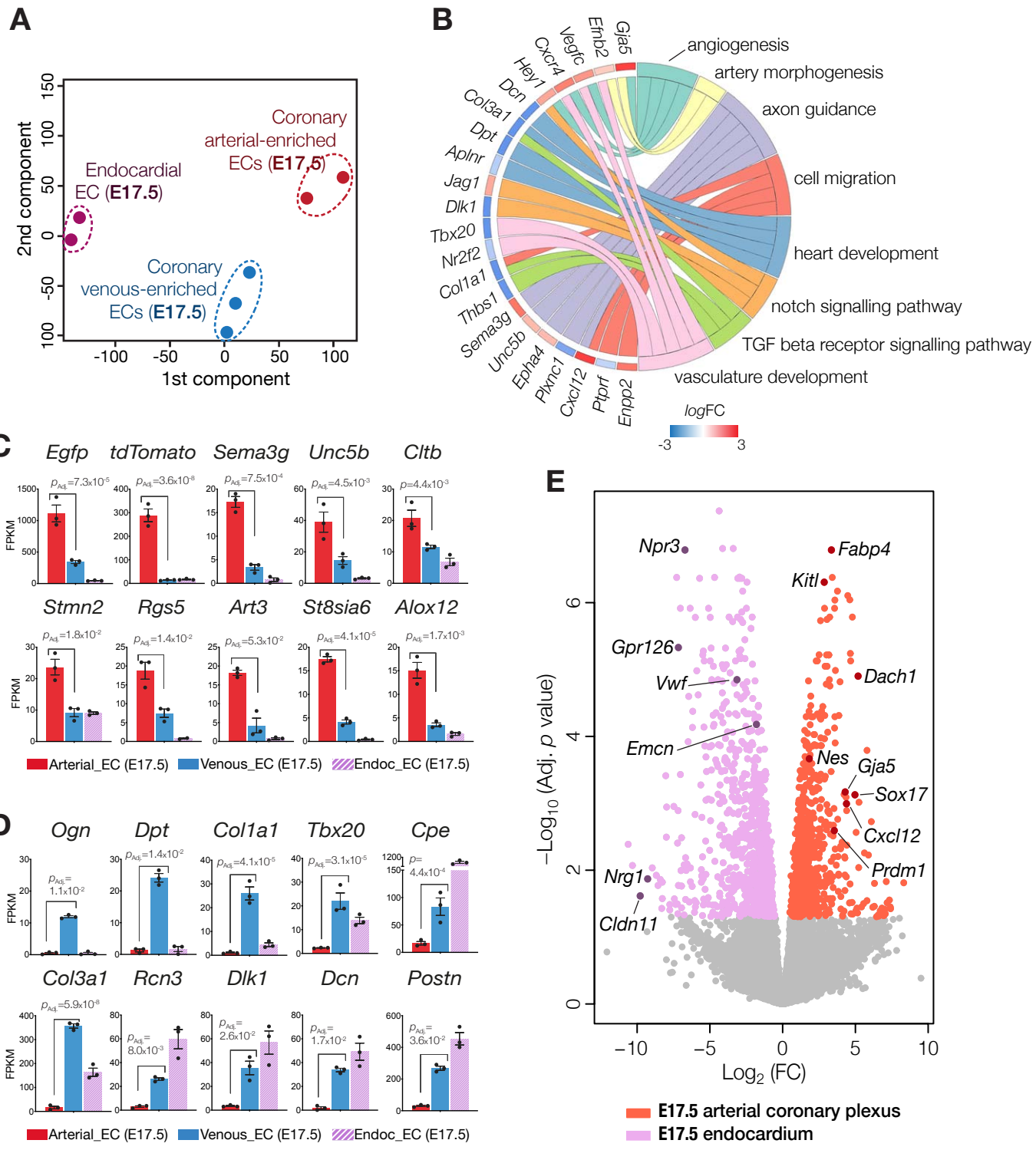
A
2nd component
1st component
Endocardial EC (E17.5)
Coronary arterial-enriched ECs (E17.5)
Coronary venous-enriched ECs (E17.5)
B
angiogenesis
artery morphogenesis
axon guidance
cell migration
heart development
notch signalling pathway
TGF beta receptor signalling pathway
vasculature development
logFC
Gja5
Efnb2
Vegfc
Cxcr4
Hey1
Dcn
Col3a1
Dpt
Aplnr
Jag1
Dlk1
Tbx20
Nr2f2
Col1a1
Thbs1
Sema3g
Unc5b
Epha4
Plxnc1
Cxcl12
Ptprf
Enpp2
C
Egfp
tdTomato
Sema3g
Unc5b
Cltb
Stmn2
Rgs5
Art3
St8sia6
Alox12
FPKM
Arterial_EC (E17.5)
Venous_EC (E17.5)
Endoc_EC (E17.5)
D
Ogn
Dpt
Col1a1
Tbx20
Cpe
Col3a1
Rcn3
Dlk1
Dcn
Postn
FPKM
Arterial_EC (E17.5)
Venous_EC (E17.5)
Endoc_EC (E17.5)
E
Npr3
Fabp4
Kitl
Gpr126
Dach1
Vwf
Emcn
Nes
Gja5
Sox17
Cxcl12
Prdm1
Nrg1
Cldn11
−Log10 (Adj. p value)
Log2 (FC)
E17.5 arterial coronary plexus
E17.5 endocardium

Figure 6

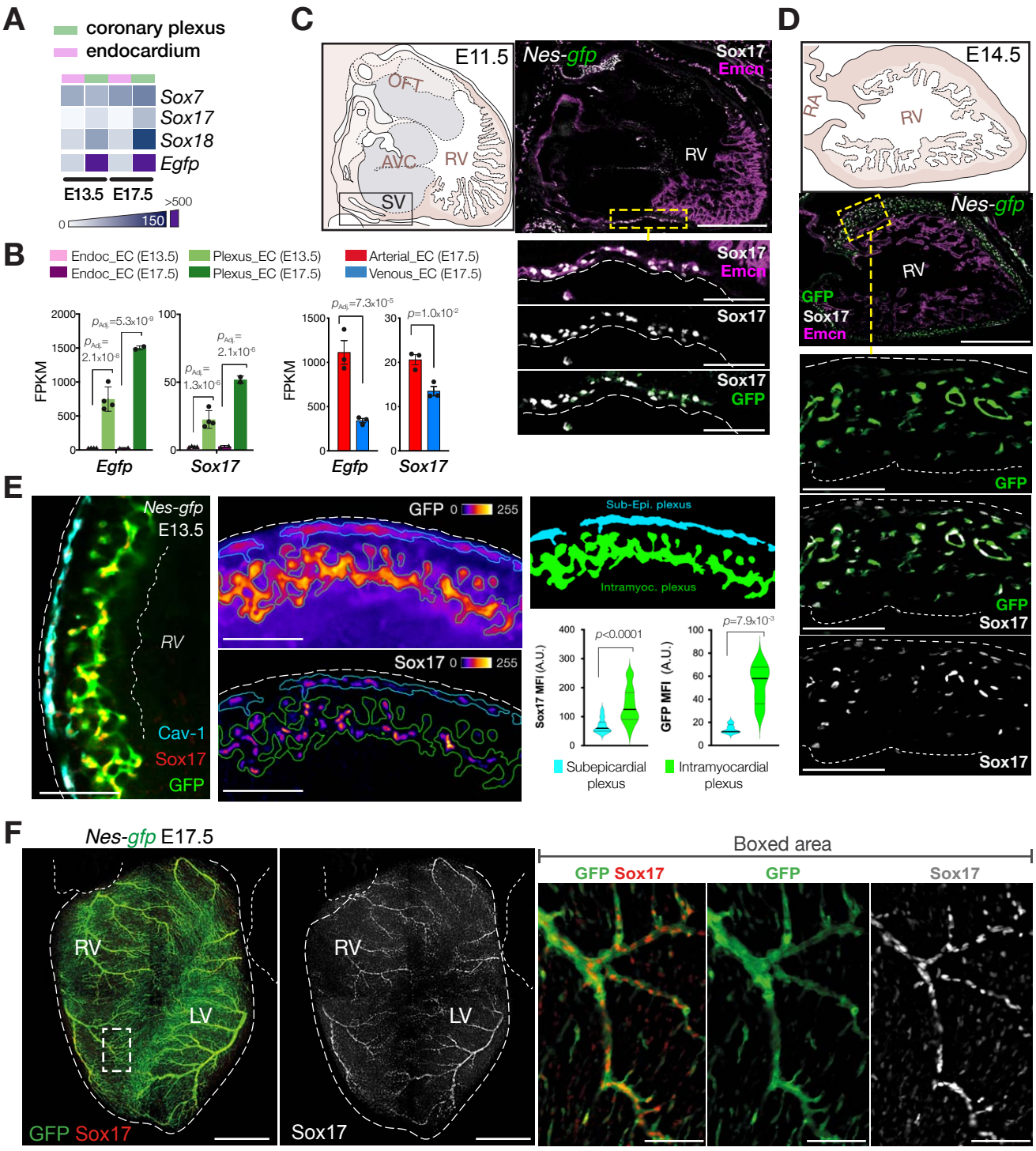
A
coronary plexus
endocardium
Sox7
Sox17
Sox18
Egfp
E13.5 E17.5
>500
0
150
B
Endoc_EC (E13.5)
Endoc_EC (E17.5)
Plexus_EC (E13.5)
Plexus_EC (E17.5)
Arterial_EC (E17.5)
Venous_EC (E17.5)
FPKM
Egfp
Sox17
C
E11.5
OFT
AVC
RV
SV
Nes-gfp
Sox17
Emcn
GFP
D
E14.5
RA
RV
E
Nes-gfp
E13.5
RV
Cav-1
Sox17
GFP
Sub-Epi. plexus
Intramyoc. plexus
Sox17 MFI (A.U.)
GFP MFI (A.U.)
Subepicardial plexus
Intramyocardial plexus
F
Nes-gfp E17.5
RV
LV
GFP Sox17
Sox17
Boxed area
GFP Sox17
GFP
Sox17

Figure 7

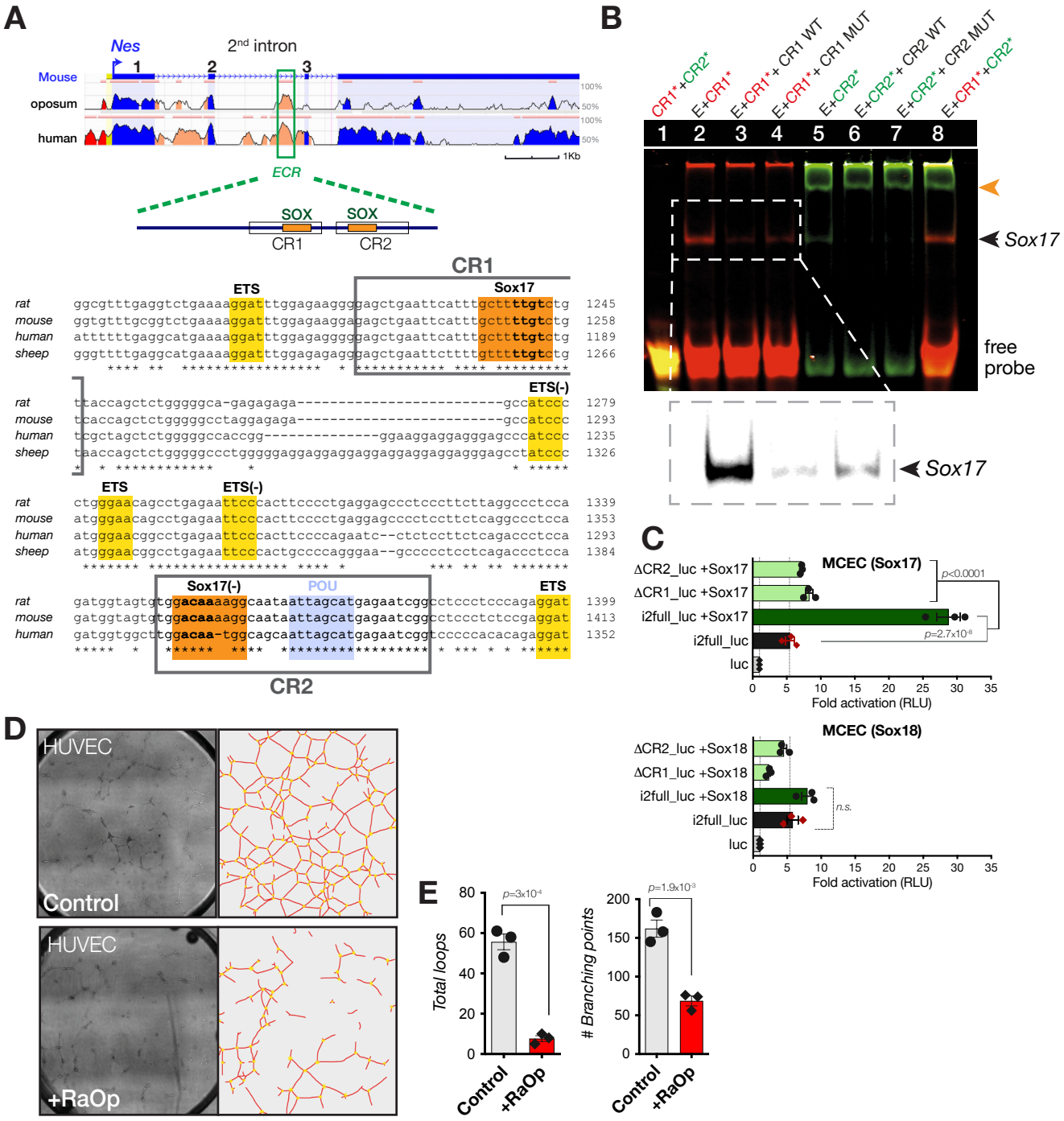
A
Nes
2nd intron
Mouse
oposum
human
ECR
SOX
SOX
CR1
CR2
CR1
ETS
Sox17
ETS(-)
ETS
ETS(-)
Sox17(-)
POU
ETS
CR2
B
CR1*+CR2*
E+CR1*
E+CR1*+ CR1 WT
E+CR1*+ CR1 MUT
E+CR2*
E+CR2*+ CR2 WT
E+CR2*+ CR2 MUT
E+CR1*+CR2*
1 2 3 4 5 6 7 8
Sox17
free probe
Sox17
C
MCEC (Sox17)
ΔCR2_luc +Sox17
ΔCR1_luc +Sox17
i2full_luc +Sox17
i2full_luc
luc
p<0.0001
p=2.7x10-8
Fold activation (RLU)
MCEC (Sox18)
ΔCR2_luc +Sox18
ΔCR1_luc +Sox18
i2full_luc +Sox18
i2full_luc
luc
n.s.
Fold activation (RLU)
D
HUVEC
Control
HUVEC
+RaOp
E
Total loops
p=3x10-4
Control
+RaOp
# Branching points
p=1.9x10-3
Control
+RaOp